applied sciences

IMPACT FACTOR 2.5

CITESCORE 5.5

Review

Quantum-Enhanced Sensing with Squeezed Light: From Fundamentals to Applications

Xing Heng, Lingchen Zhang, Qingyun Yin, Wei Liu, Lulu Tang, Yueyang Zhai and Kai Wei

Special Issue

Precision Measurement Technology

Edited by

Dr. Mohammed A. Isa, Dr. Mingyu Liu and Prof. Dr. Samanta Piano

MDPI

https://doi.org/10.3390/app151810179

applied sciences

MDPI

Review

Quantum-Enhanced Sensing with Squeezed Light: From Fundamentals to Applications

Xing Heng [1,2,3,*], Lingchen Zhang [2,3], Qingyun Yin [2,3], Wei Liu [4], Lulu Tang [4], Yueyang Zhai [1,2,3,4,5] and Kai Wei [1,2,3,4,5,*]

1 School of Instrumentation and Optoelectronic Engineering, Beihang University, Beijing 100191, China
2 Institute of Large-Scale Scientific Facility, Beihang University, Beijing 100191, China
3 Hangzhou Innovation Institute, Beihang University, Hangzhou 310051, China
4 Hangzhou Institute of Extremely-Weak Magnetic Field Major National Science and Technology Infrastructure, Hangzhou 310051, China
5 Hefei National Laboratory, Hefei 230088, China
* Correspondence: xingheng@buaa.edu.cn (X.H.); weikai@buaa.edu.cn (K.W.)

Abstract

Squeezed light, a prominent non-classical state of light, exhibits reduced quantum noise in one quadrature component below the standard quantum limit (SQL). The property enables quantum-enhanced precision measurements, surpassing the SQL in quantum sensing applications. This review comprehensively introduces the fundamental concepts, classifications, and experimental generation techniques of squeezed light. It further explores its pivotal role and recent advances in diverse quantum sensing domains, including interferometry, gravitational wave detection, magnetometry, force sensing, biomedical sensing, and quantum radar. The review covers theoretical foundations of squeezed states (including quadrature operators and classification schemes, experimental generation techniques in atomic ensembles, nonlinear crystals, and fibers), fundamentals of quantum sensing with squeezed light (from quantum noise theory to quantum-enhanced metrology), and quantum-enhanced sensing applications across the aforementioned domains. Finally, future challenges and opportunities in the field are discussed.

Keywords: squeezed light; quantum sensing; quantum information; quantum metrology

Academic Editors: Durdu Guney and Vladimir M. Fomin

Received: 19 August 2025
Revised: 5 September 2025
Accepted: 16 September 2025
Published: 18 September 2025

Citation: Heng, X.; Zhang, L.; Yin, Q.; Liu, W.; Tang, L.; Zhai, Y.; Wei, K. Quantum-Enhanced Sensing with Squeezed Light: From Fundamentals to Applications. *Appl. Sci.* **2025**, *15*, 10179. https://doi.org/10.3390/app151810179

1. Introduction

As classical techniques approach fundamental limitations, quantum technologies are demonstrating significant advantages across diverse domains [1,2]. Key applications leverage quantum resources—such as coherence [3], entanglement [4], and interference [5]—to enhance sensitivity and resolution in sensing [6–8] and imaging [9,10], surpassing the capabilities of classical methods. Beyond these core domains, quantum sensors enabled by squeezed light hold promise for transformative applications in medical diagnosis, atmospheric sensing, and navigation systems [6,8]. In healthcare, they facilitate early disease detection through non-invasive imaging and biomarker identification, potentially revolutionizing diagnostics [11]. For environmental monitoring, quantum sensors can identify pollutants with unprecedented precision and contribute accurate data to climate models [7]. Furthermore, advancements in quantum sensing increasingly intersect with quantum computing and communication, enabling hybrid systems for distributed networks and enhanced information security [12].

Many high-precision sensors utilize atomic systems with optical readout, where quantum noise intrinsic to light–atom interactions imposes a fundamental constraint on measurement accuracy, known as the standard quantum limit (SQL) [13,14]. In optical interferometry, for instance, vacuum fluctuations of the electromagnetic field manifest as a dominant quantum noise source, establishing the SQL for phase measurement sensitivity, which scales as $1/\sqrt{N}$ (where N is the average photon number) [15]. This represents the optimal sensitivity typically attainable using classical light sources.

To surpass the SQL, non-classical states of light—including entangled states [16], squeezed states [17], single-photon states [18], Schrödinger-cat states [19], and NOON states [20]—have been developed and experimentally verified. Beyond enhanced metrology, quantum light offers distinct advantages for quantum information processing, such as increased information capacity, faster processing, and inherent security [21,22]. Furthermore, foundational tests of quantum mechanics, including Einstein–Podolsky–Rosen (EPR) entanglement [23], quantum non-locality [24], and Bell inequality violations [25], are critically reliant on these non-classical states.

Among these, squeezed light is a quintessential non-classical state characterized by quantum noise reduction below the SQL in one quadrature component. This unique property makes it exceptionally promising for achieving quantum-enhanced sensitivity in sensing applications [26–28]. Indeed, squeezed-light-enhanced measurements have now been successfully demonstrated in diverse fields, including magnetometers [29,30], phase estimation [31,32], gravitational wave detection [33,34], and quantum illumination radar [28,35]. In quantum information, the complex photon number distributions inherent to squeezed states provide computational advantages, exemplified in Gaussian boson sampling [36]. Consequently, squeezed light is revolutionizing the achievable scales and precision in both sensing [37,38] and imaging [39,40].

Motivated by the growing demand for precision beyond classical limits in fields like astrophysics [41], biomedical diagnostics [42], and secure communication [43], this review focuses on the pivotal role of squeezed light in advancing quantum sensing. We begin by outlining the fundamental principles of squeezed states and detailing key experimental generation methods, such as four-wave mixing (FWM) and polarization self-rotation (PSR) in atomic ensembles, parametric down-conversion (PDC) in nonlinear crystals, and the optical Kerr effect in fibers. Subsequently, we comprehensively survey applications in quantum sensing, encompassing interferometry, gravitational wave detection, magnetometry, bio-sensing, force sensing, radar, and ranging.

2. Principles in Squeezed Light

2.1. Basic Properties of Squeezed Light

The photon creation operator $\hat{a}^\dagger$ and the annihilation operator $\hat{a}$ are non-Hermitian and therefore do not correspond to directly measurable observables in quantum mechanics. The Hermitian quadrature operators, which represent the measurable amplitude and phase components of the quantized electromagnetic field, are defined as

$$\begin{cases} \hat{X} = \dfrac{\hat{a} + \hat{a}^\dagger}{2} \\ \hat{Y} = \dfrac{\hat{a} - \hat{a}^\dagger}{2i} \end{cases} \tag{1}$$

In the Heisenberg picture, the time evolution of the annihilation operator for a mode of frequency ω is given by the following:

$$\begin{cases} \hat{a}(t) = \hat{a} \cdot e^{-i\omega t} \\ \hat{a}^{\dagger}(t) = \hat{a}^{\dagger} \cdot e^{i\omega t} \end{cases} \tag{2}$$

The quantized electric field for a monochromatic wave of frequency ω, wave number k, and amplitude E_0 can be expressed as

$$\hat{E}(z,t) = 2E_0 \sin(kz)\left[\hat{X}\cos(\omega t) + \hat{Y}\sin(\omega t)\right] \tag{3}$$

The fluctuations of the quadrature operators $\Delta\hat{X} = \hat{X} - \langle\hat{X}\rangle$ and $\Delta\hat{Y} = \hat{Y} - \langle\hat{Y}\rangle$ are constrained by the Heisenberg uncertainty principle:

$$\left\langle(\Delta\hat{X})^2\right\rangle\left\langle(\Delta\hat{Y})^2\right\rangle \geq \frac{1}{16} \tag{4}$$

where $\langle(\Delta\hat{O})^2\rangle$ denotes the variance of operator $\hat{O}$. This implies that $\hat{X}$ and $\hat{Y}$ cannot simultaneously have arbitrarily small uncertainties.

For both the vacuum state $|0\rangle$ and a coherent state $|\alpha\rangle$, the quadrature variances reach the minimum uncertainty product:

$$\left\langle(\Delta\hat{X})^2\right\rangle = \left\langle(\Delta\hat{Y})^2\right\rangle = \frac{1}{4} \tag{5}$$

This minimum uncertainty level, inherent to coherent states and the vacuum, defines the standard quantum limit (SQL) for phase and amplitude measurements using classical light sources.

A squeezed state can be generated by applying the squeezing operator $\hat{S}(\xi)$ to a coherent state (or the vacuum state). Here, $\xi = re^{i\theta}$ is the complex squeezing parameter, with $r \geq 0$ representing the squeezing strength and $\theta \in [0, 2\pi)$ the squeezing angle determining the quadrature axis of noise reduction. In a squeezed state, the variances of the quadrature operators become

$$\begin{cases} \left\langle(\Delta\hat{X})^2\right\rangle = \dfrac{e^{-2r}\cos^2\theta + e^{2r}\sin^2\theta}{4} \\ \left\langle(\Delta\hat{Y})^2\right\rangle = \dfrac{e^{-2r}\sin^2\theta + e^{2r}\cos^2\theta}{4} \end{cases} \tag{6}$$

Crucially, for specific phases (θ), the variance of one quadrature component ($\hat{X}$ or $\hat{Y}$) is reduced below the SQL value of $1/4$, at the expense of increased noise in the conjugate quadrature. This phenomenon, where quantum noise in one observable is "squeezed" below the vacuum level, is the defining characteristic of squeezed light. Figure 1 illustrates the phase-space representations of key states: (a, d) coherent state (circular noise distribution), (b, e) phase-squeezed state ($\theta = \pi/2$, noise reduced in $\hat{Y}$), and (c, f) amplitude-squeezed state ($\theta = 0$; noise reduced in $\hat{X}$).

The noise redistribution property of squeezed light (Equation (6)) provides a critical advantage for quantum sensing. By reducing noise in a specific quadrature below the SQL, it enables parameter estimation precision beyond classical limits. For example, in phase sensing, a phase-squeezed state suppresses noise in the measurement quadrature [44]. In absorption measurements, amplitude squeezing enhances intensity detection sensitivity [40]. This intrinsic noise engineering capability makes squeezed light superior to classical states (such as coherent states of less structured light) for overcoming quantum noise barriers in high-precision measurements, as will be demonstrated in Section 3 applications.

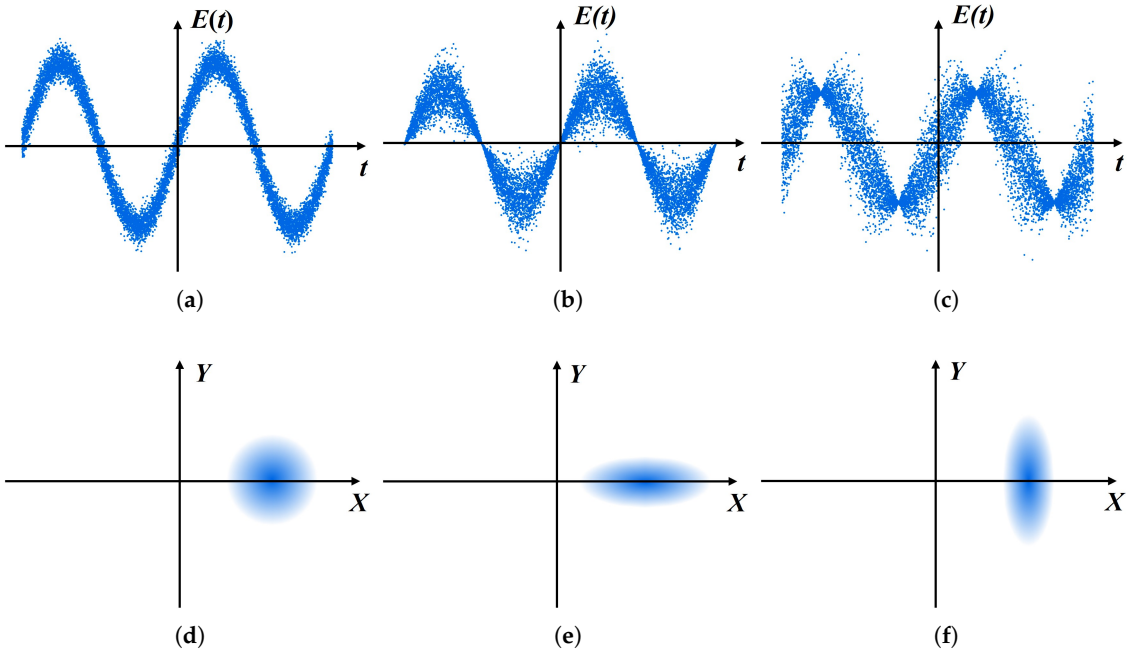

Figure 1. Quantum noise characteristics in time and phase space. (**a**) Temporal quantum noise of a coherent state (electric field amplitude vs. time). (**b**) Temporal quantum noise of a phase-squeezed state. (**c**) Temporal quantum noise of an amplitude-squeezed state. (**d**) Phase-space representation of a coherent state. (**e**) Phase-space representation of a phase-squeezed state. (**f**) Phase-space representation of an amplitude-squeezed state.

2.2. Classification of Squeezed Light

2.2.1. Quadrature-Squeezed States

The coherent state is a minimum-uncertainty state with equal fluctuations in both quadrature components ($\hat{X}$ and $\hat{Y}$). A quadrature-squeezed state is defined as a state where the variance of one quadrature component is reduced below the coherent-state level (i.e., below the SQL of 1/4), while satisfying the Heisenberg uncertainty principle by exhibiting increased noise in the conjugate quadrature.

Based on the number of optical modes involved, quadrature-squeezed states are categorized as single-mode squeezed states, two-mode squeezed states, and multimode squeezed states.

Single-mode squeezed states are generated by applying the squeezing operator $\hat{S}(\xi)$ to a single-mode coherent state:

$$|\alpha, \xi\rangle_{\mathrm{SMSS}} = \hat{D}(\alpha, \alpha^*)\hat{S}(\xi)|0\rangle \tag{7}$$

where $\hat{D}(\alpha, \alpha^*) = \exp(\alpha\hat{a}^\dagger - \alpha^*\hat{a})$ is the displacement operator, and $\hat{S}(\xi) = \exp[(\xi\hat{a}^{\dagger 2} - \xi^*\hat{a}^2)/2]$ is the single-mode squeezing operator. Single-mode squeezed states in quantum optics are typically generated through processes that reduce quantum noise in one quadrature of the electromagnetic field at the expense of increasing it in the conjugate quadrature, often using nonlinear optical interactions [45].

Two-mode squeezed states, also known as twin-beam or Einstein–Podolsky–Rosen (EPR) entangled states, involve two independent optical modes, described by two independent operators ($\hat{a}_1$, $\hat{a}_1^\dagger$ and $\hat{a}_2$, $\hat{a}_2^\dagger$) satisfying $[\hat{a}_i, \hat{a}_j^\dagger] = \delta_{ij}$ $(i, j = 1, 2)$. The two-mode squeezed vacuum state is generated by

$$|\xi\rangle_{\mathrm{TMSS}} = \hat{T}(\xi)|0, 0\rangle \tag{8}$$

where $\hat{T}(\xi) = \exp(\xi \hat{a}_1^\dagger \hat{a}_2^\dagger - \xi^* \hat{a}_1 \hat{a}_2)$ is the two-mode squeezing operator. This state exhibits quantum correlations between the modes. A displaced two-mode squeezed state is

$$|\alpha_1, \alpha_2, \xi\rangle_{\text{TMSS}} = \hat{D}_1(\alpha_1)\hat{D}_2(\alpha_2)\hat{T}(\xi)|0,0\rangle \tag{9}$$

Two-mode squeezed states are produced by correlating quantum fluctuations between two distinct optical modes, often spatial, temporal, or polarization modes, leading to entanglement and squeezing in joint quadratures [46,47].

Multimode squeezed states extend squeezing and entanglement across more than two modes, enabling scalable quantum networks [48] and enhanced metrology by distributing quantum resources over frequency, time, or spatial domains [49].

2.2.2. Photon-Number-Squeezed States

The photon number operator $\hat{n}$ and phase operator $\hat{\phi}$ are also a pair of conjugated quantities, satisfying the Heisenberg uncertainty relationship:

$$\langle (\Delta\hat{n})^2 \rangle \langle (\Delta\hat{\phi})^2 \rangle \geq \frac{1}{16} \tag{10}$$

Photon-number-squeezed states have reduced photon number fluctuations ($(\Delta\hat{n})^2 < \langle\hat{n}\rangle$) compared to the coherent states (which exhibit Poissonian statistics with $(\Delta\hat{n})^2 = \langle\hat{n}\rangle$). Therefore, the photon number-squeezed light is referred to as sub-Poissonian light as well, and can be generated via nonlinear processes (e.g., in a Mach–Zehnder interferometer with Kerr nonlinearity [50,51]), offering potential advantages in low-noise communication.

2.2.3. Intensity-Difference-Squeezed States

The intensity-difference-squeezed state is a specific two-mode state where the variance of the photon number difference operator $\Delta(\hat{n}_1 - \hat{n}_2)^2$ falls below the SQL (which would be the shot-noise level for two independent coherent states). Intensity-difference-squeezed states exhibit strong quantum intensity correlations between the two modes (often called "twin beams"). The twin beams are experimentally robust and show potential applications in quantum imaging [52,53], quantum random number generation [54,55], and quantum non-demolition measurements [56].

2.3. Experimental Generation of Squeezed Light

The experimental realization of squeezed states of light relies fundamentally on harnessing optical nonlinearities—predominantly second-order ($\chi^{(2)}$) and third-order ($\chi^{(3)}$) nonlinear processes—that arise during the interaction of intense light fields with various media. Key platforms for generating squeezed light include atomic vapors, nonlinear crystals, and optical fibers, with each one exploiting distinct physical mechanisms.

2.3.1. Atomic Ensembles

Dense atomic vapors provide a versatile medium for squeezed light generation primarily through strong nonlinearities. The polarization self-rotation (PSR) effect and four-wave mixing (FWM) process are two principal mechanisms that are employed.

1. Polarization self-rotation

When linearly polarized light propagates through an atomic vapor, quantum vacuum fluctuations in the orthogonal polarization component induce a weak nonlinear birefringence. This effect, known as polarization self-rotation, redistributes quantum noise, leading to quadrature squeezing in the initially unpopulated orthogonal polarization mode (Figure 2a). Balanced homodyne detection (BHD), involving interference with a strong

local oscillator field and phase scanning, is used to characterize the squeezed quadrature variance. While theoretical models predict achievable squeezing levels near 6 dB in rubidium vapor [57], experimental demonstrations using PSR have typically yielded around 3 dB of measured squeezing [58–60]. Recent advancements, such as the application of a weak transverse magnetic field, have enhanced this performance, achieving 3.5 ± 0.2 dB of directly measured squeezing (equivalent to 4.2 ± 0.2 dB after correction for optical losses) [61].

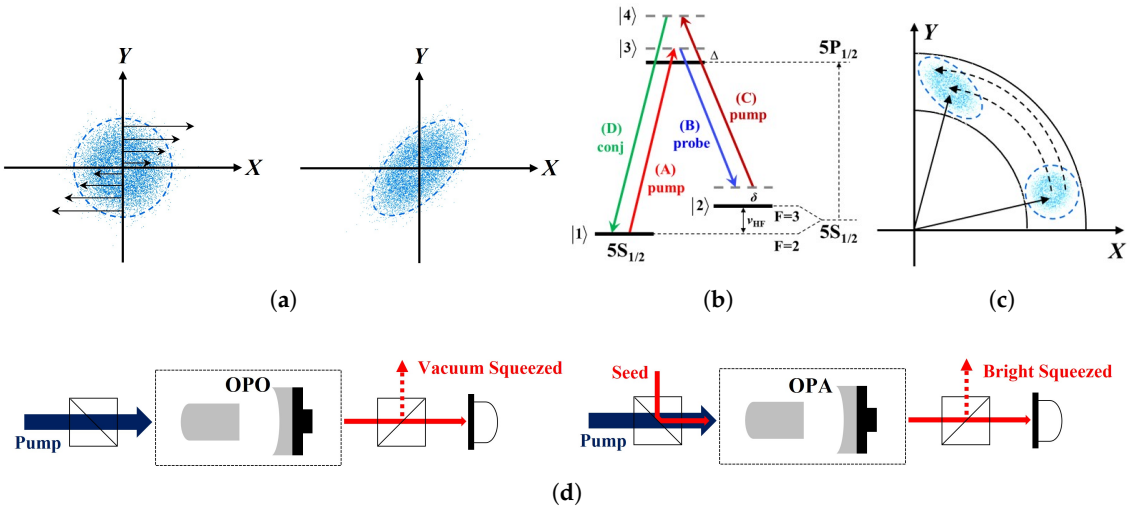

Figure 2. Schematic diagram of several preparation methods for squeezed light. (**a**) The process by which polarization self-rotation (PSR) leads to a vacuum-squeezed state. (**b**) Energy levels in double-Λ shape in process of four-wave mixing (FWM). (**c**) Squeezing of a coherent state by the nonlinear optical Kerr effect in quadrature phase space. (**d**) Experimental designs of optical parametric oscillation (OPO) and optical parametric amplification (OPA).

2. Four-wave mixing

Resonant FWM processes leverage intense $\chi^{(3)}$ nonlinearities near atomic transitions, where two pump photons are annihilated to create correlated signal and idler photon pairs. This process inherently generates two-mode squeezed states, manifesting as intensity-difference squeezing between the signal and idler beams. The landmark experimental demonstration of squeezed light by Slusher et al. in 1985 achieved 0.3 dB of squeezing via cavity-enhanced FWM in sodium vapor [62]. A highly efficient configuration utilizes the double-Λ atomic energy level scheme (Figure 2b), which has been extensively studied in rubidium vapor. McCormick et al. utilized this scheme to demonstrate 3.5 dB of intensity-difference squeezing [63], which subsequently improved to 8.8 dB through careful optimization of pump and probe beam parameters [64]. Recent research has focused on achieving stable squeezing at low frequencies, successfully demonstrating over 5 dB of intensity-difference squeezing below 20 Hz in FWM-generated twin beams [40,65]. The current record for squeezing generated within an atomic ensemble stands at 9.2 dB of intensity-difference squeezing [66]. A significant challenge in resonant FWM is optical loss due to atomic absorption [67,68]. Mitigation strategies include exploiting isotopic shifts (e.g., generating ^{87}Rb-resonant twin beams within a ^{85}Rb vapor cell [69,70]) or employing coherent population trapping (CPT) in metastable helium at room temperature [71]. CPT creates a narrow transparency window within the absorption profile, enabling efficient FWM near resonance by suppressing absorption losses.

2.3.2. Nonlinear Crystals

Ferroelectric nonlinear crystals with large second-order ($\chi^{(2)}$) nonlinear coefficients enable highly efficient squeezed light generation through parametric down-conversion (PDC) processes, typically implemented in resonant optical cavities. There are two primary configurations: optical parametric oscillation (OPO) and optical parametric amplification (OPA).

In OPO process, pump light is injected into a nonlinear crystal placed inside an optical cavity operating below its oscillation threshold. The PDC process spontaneously generates correlated signal and idler photons from the pump vacuum fluctuations, resulting in a vacuum squeezed state at the output. The intensity difference between the signal and idler modes exhibits quantum noise reduction below the shot-noise level.

However, during the OPA process, a seed beam (at either the signal or idler frequency) is co-injected with the pump into the nonlinear medium within a cavity. The seed beam experiences amplification, and the output constitutes a bright squeezed state. OPA circumvents the oscillation threshold requirement of OPO but often necessitates an optical cavity to achieve sufficient nonlinear interaction strength for high squeezing levels.

Materials like magnesium oxide-doped lithium niobate (MgO:$LiNbO_3$) and periodically poled potassium titanyl phosphate (PPKTP) exhibit exceptionally high nonlinear conversion efficiencies. Continuous refinement of cavity-enhanced PDC techniques in these crystals has driven a steady progression in achievable squeezing levels. The pioneering work by Wu et al. demonstrated 3.5 dB of squeezing using MgO:$LiNbO_3$ in a cavity [72]. Significant improvements followed, achieving 6.0 ± 0.25 dB [73] and 7 dB [74] of squeezing, largely attributed to reductions in intracavity optical losses via improved crystal coating and monolithic cavity designs. Further minimization of cavity losses and enhanced phase locking stability allowed the observation of 9 dB squeezing [75]. The implementation of cavity filtering techniques to suppress phase noise from the pump laser facilitated the measurement of 10 dB squeezing [76]. Utilizing homodyne detectors with higher quantum efficiency [77] yielded 11.6 dB of squeezing [78]. Advanced cavity configurations, such as double-resonant OPA employing PPKTP crystals, achieved 12.7 dB squeezing [26]. The current state-of-the-art stands at 15 dB of squeezing at 1064 nm [79], a wavelength that is critically important for gravitational wave interferometers. Concurrently, significant progress has been made in the telecommunications band (1550 nm) [80], where squeezing levels exceeding 12 dB have been reported [81–83].

2.3.3. Optical Fibers

Squeezed light generation in optical fibers exploits the optical Kerr effect, a third-order ($\chi^{(3)}$) nonlinearity. An intense coherent laser beam propagating through the fiber induces an intensity-dependent nonlinear phase shift (self-phase modulation) via the Kerr nonlinearity. This deterministic phase modulation redistributes quantum noise between the field quadratures, potentially leading to quadrature squeezing in the output [84] (Figure 2c). Optical fibers offer significant advantages, including low propagation loss over extended interaction lengths and the absence of stringent phase-matching requirements inherent to $\chi^{(2)}$ processes. However, detrimental nonlinear effects, particularly stimulated Brillouin scattering (SBS), introduce significant excess noise in response to high optical power and limit the practically usable fiber length and pump intensity [85].

The initial realization in 1986 achieved 0.6 dB of squeezing using a 114 m fiber cooled to 4.2 K and high-power continuous-wave (CW) laser light [86]. Employing pulsed lasers instead of CW sources yielded 1.1 dB squeezing [87]. A compact setup on a 0.3 m^2 platform generated 2.4 dB of pulsed squeezing [88]. Using ultrashort pulses (140 fs full width at half maximum—FWHM) in polarization-maintaining fiber enabled 6.8 dB squeezing [89]. The-

oretical studies predict the potential for greater than 10 dB squeezing at 2 μm wavelengths using specialized chalcogenide glass fibers designed for enhanced Kerr nonlinearity [90].

3. Fundamentals of Quantum Sensing with Squeezed Light

The strategic implementation of squeezed light in quantum sensing aims to circumvent fundamental quantum noise limitations inherent in precision optical measurements. By engineering non-classical correlations within the electromagnetic field, squeezed states enable measurement sensitivities beyond the SQL. This section establishes a theoretical framework detailing the quantum mechanical origins of measurement noise, elucidates the physical mechanism through which squeezed light redistributes quantum fluctuations, and quantifies the resultant metrological enhancement. Interferometric phase estimation serves as our paradigmatic model throughout this exposition, given its centrality in quantum metrology [91].

3.1. Quantum Noise in Optical Precision Measurements

Optical precision measurements encounter irreducible constraints imposed by quantum mechanical uncertainties. Shot noise and vacuum fluctuation noise are two primary noise manifestations that dominate.

Shot noise, arising from the Poissonian photon statistics of coherent states, establishes the SQL for phase estimation. For a probe field containing $\langle n \rangle$ photons on average, the minimum achievable phase uncertainty is constrained to $\Delta\phi_{\mathrm{SQL}} = 1/\sqrt{\langle n \rangle}$. The quantum noise fundamentally stems from the discrete nature of photon detection events and represents the ultimate sensitivity limit for classical light sources.

Concurrently, vacuum fluctuation noise imposes critical limitations in interferometric architectures. When vacuum states enter unused optical ports—as occurs in balanced interferometers—their quantum fluctuations propagate through beam-splitting transformations [92]. The vacuum quadrature variances $\langle (\Delta\hat{X})^2 \rangle = \langle (\Delta\hat{Y})^2 \rangle = 1/4$, saturating the Heisenberg uncertainty principle $\langle (\Delta\hat{X})^2 \rangle \langle (\Delta\hat{Y})^2 \rangle = 1/16$, establish the SQL in such configurations. These combined quantum noise sources impose fundamental sensitivity ceilings across diverse applications, from gravitational-wave interferometry [93,94] to optical atomic clocks [95].

3.2. Noise-Reduction Mechanism of Squeezed States

Squeezed light overcomes SQL constraints through controlled redistribution of quantum fluctuations across conjugate field quadratures. The quadrature operators described in Equation (1) exhibit asymmetric variances in squeezed states:

$$\begin{cases} \langle (\Delta\hat{X})^2 \rangle = \dfrac{e^{-2r}}{4} \\ \langle (\Delta\hat{Y})^2 \rangle = \dfrac{e^{2r}}{4} \end{cases} \tag{11}$$

where $r \geq 0$ denotes the squeezing parameter. The noise anisotropy preserves the Heisenberg uncertainty principle while enabling phase-dependent noise suppression.

The underlying mechanism for metrological enhancement is illustrated in interferometric configurations. Injection of a phase-squeezed vacuum ($\theta = \pi/2$) into the dark port replaces vacuum fluctuations with correlated noise [92]. Alignment of the squeezed quadrature with the phase-sensitive output quadrature reduces its noise variance from $1/4$ to $e^{-2r}/4$. Consequently, the signal-to-noise ratio for phase-shift detection improves without signal amplification, constituting a quintessential quantum advantage.

3.3. Quantitative Enhancements and Limitations

The phase uncertainty achievable with squeezed-light injection is as follows:

$$\Delta\phi = \frac{e^{-r}}{\sqrt{\langle n \rangle}} \tag{12}$$

yielding a quantum enhancement factor

$$\mathcal{Q} = \frac{\Delta\phi_{\mathrm{SQL}}}{\Delta\phi} = e^{r} \tag{13}$$

Experimentally demonstrated squeezing levels of 10 dB (corresponding to $r \approx 1.15$, $\mathcal{Q} \approx 3.2$) provide significant sensitivity gains, approaching the Heisenberg limit $\Delta\phi \propto 1/\langle n \rangle$ [51] at the upper squeezing range.

However, squeezed light primarily addresses quantum noise and does not mitigate classical sources (e.g., thermal noise [96] or mechanical vibrations [91]). Amplified noise in the anti-squeezed quadrature may introduce artifacts, necessitating precise phase locking [97]. Practical systems also contend with optical losses [98], which dilute squeezing and require optimization for net gains.

These principles establish the theoretical foundation for squeezed light's transformative impact in quantum-enhanced metrology. Subsequent sections detail experimental validations across gravitational-wave detectors [41], magnetometry [27], and biological sensing [99], demonstrating the translation of these quantum advantages into functional sensing platforms.

4. Applications in Quantum-Enhanced Sensing

The seminal theoretical work by Caves in 1981 established the foundation for squeezed light in quantum metrology, proposing that injecting a squeezed vacuum into an interferometer's unused port could replace vacuum fluctuations and thereby reduce measurement noise below the standard quantum limit (SQL) [92]. This insight catalyzed the integration of squeezed states into diverse quantum sensing architectures (as shown in Figure 3), demonstrating significant enhancements across multiple domains.

From a quantum information perspective, squeezed light enhances sensing by increasing the Fisher information (FI), which quantifies the amount of information about an unknown parameter (e.g., phase or magnetic field) extractable from a measurement, often leading to input/output gains that approach the Heisenberg limit [100,101]. The Holevo bound, representing the ultimate limit on accessible information in quantum channels, further elucidates how squeezed states mitigate information loss in noisy media, providing robustness at both extremes of sensing: maximal gain in ideal channels and superior performance under decoherence [102,103]. For instance, in quantum channels, squeezed light can yield up to 3 dB FI enhancement compared to coherent states, reducing estimation variance [104]. As illustrated in Figure 4, which presents numerical simulations based on theoretical scaling laws, panel (a) depicts FI as a function of photon number N (ranging from 1 to 100), contrasting the linear scaling (FI $\approx N$) for coherent states with the quadratic scaling (FI $\approx N^2$) for squeezed states, highlighting the potential for enhanced precision in parameter estimation. Panel (b) simulates the Holevo information under varying transmissivity η (from 0 to 1), using simplified models such as $-\log_2(1-\eta)$ for coherent states and $-\log_2(1-\eta^2)$ for squeezed states, to demonstrate reduced information decay and thus greater resilience to loss in squeezed-light scenarios.

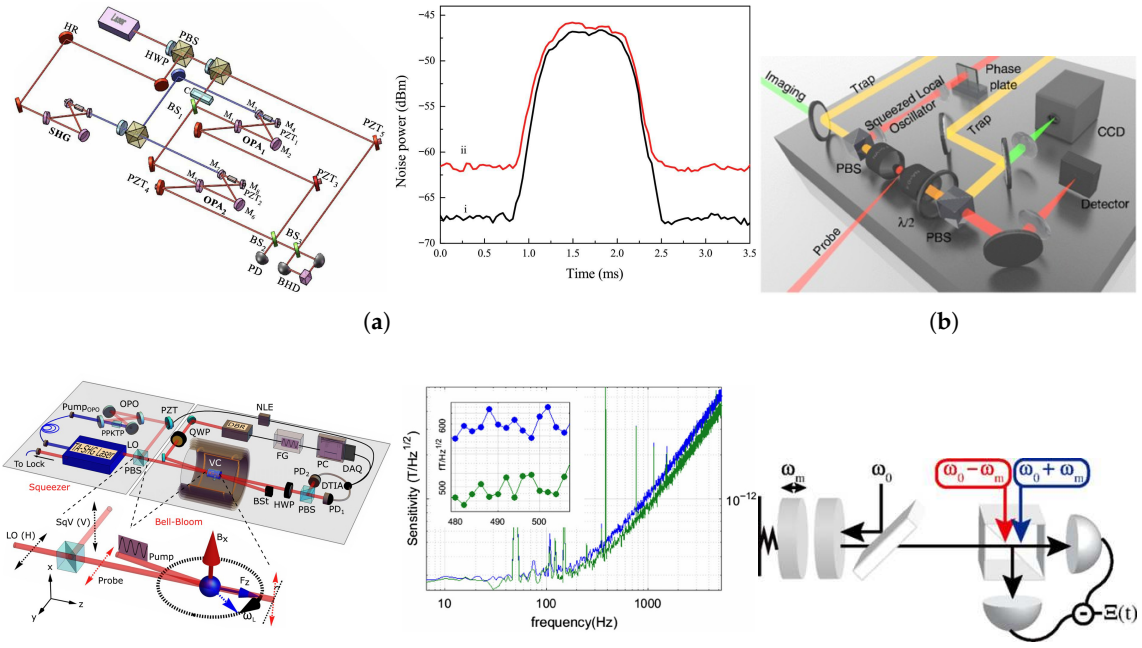

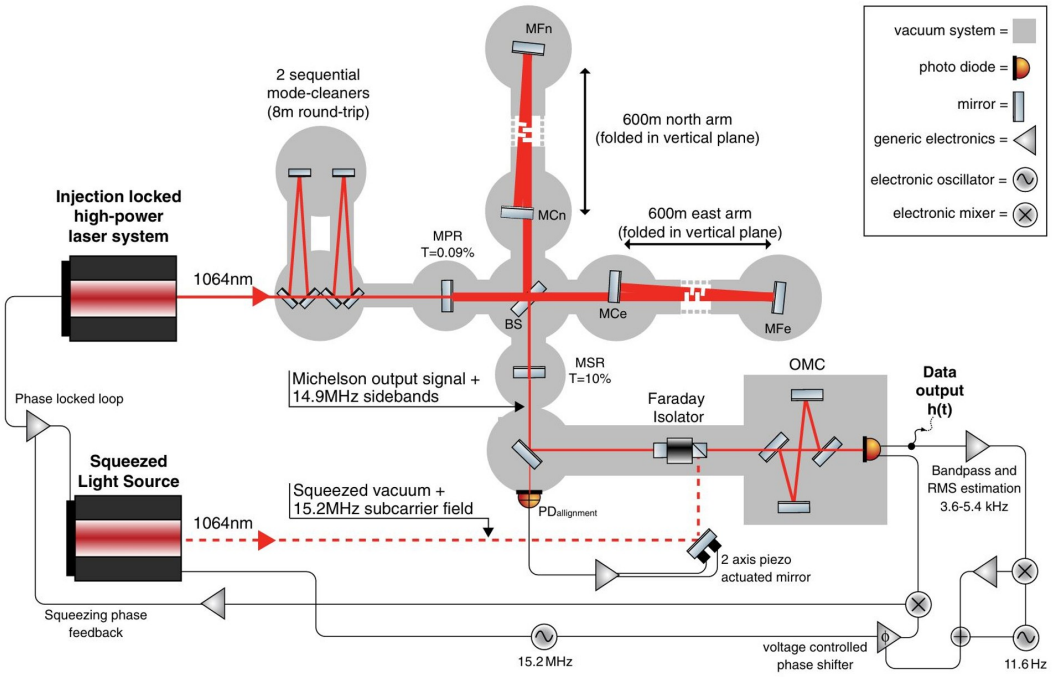

Figure 3. Quantum-enhanced sensing with squeezed light. (**a**) The experimental setup (**left**) for implementing the phase change measurement using Mach–Zehender interferometer with squeezed light. The signal and noise levels (**right**) are measured at the output field of the interferometer, where the red trace is the shot noise limit while the black trace is the output noise power measured with squeezed light. Adapted with permission from [105]. (**b**) Experimental setup of conventional photonic-force microscopy, facilitating the use of amplitude-squeezed light to enhance measurement sensitivity. Adapted with permission from [42]. (**c**) Experimental setup (**left**) of a squeezed-light Bell–Bloom optically pumped magnetometer. The Sensitivity spectra (**right**) for the Bell–Bloom magnetometer probe with coherent (blue) and squeezed light (green). Adapted with permission

from [30]. (**d**) The complex ponderomotive optical squeezing spectrum produced by cavity optomechanics is sensed by synodyne detection. Adapted with permission from [106]. (**e**) A simplified optical layout of the squeezed-light enhanced German-British detector GEO 600, which consists of the conventional GEO 600 observatory and the additional squeezed-light source. Adapted with permission from [107].

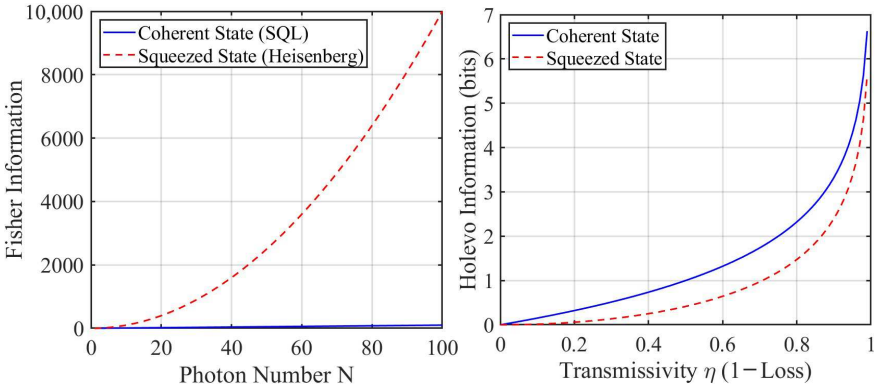

Figure 4. Schematic illustrating the relation between squeezed light and quantum information metrics in sensing. (**a**) Fisher information scaling for phase estimation, contrasting coherent states (bounded by the standard quantum limit) with squeezed states (approaching Heisenberg-like potential). (**b**) Holevo bound under channel loss, depicting reduced information decay for squeezed inputs versus classical light. This graphical representation highlights input/output gains and performance under loss.

4.1. Interferometry

Interferometric precision, fundamentally limited by quantum noise, benefits profoundly from squeezed light injection. Building on Caves' proposal, early experimental demonstrations by Xiao et al. [108] and Slusher et al. [109] achieved phase measurement sensitivities surpassing the SQL within Mach–Zehnder and polarization interferometers, reporting signal-to-noise ratio (SNR) enhancements of 3 dB and 2 dB, respectively. These results validated the core concept of quantum noise suppression via squeezed vacuum. Further theoretical and experimental advances explored the potential of non-Gaussian states like NOON states to approach the Heisenberg limit in sensitivity [110,111]. A significant development emerged with the SU(1,1) interferometer, where linear beam splitters are replaced by nonlinear optical parametric amplifiers (OPAs). This configuration intrinsically amplifies the signal while maintaining noise levels, yielding a phase sensitivity enhancement proportional to the interferometer gain [31,44]. Hudelist et al. experimentally realized a nonlinear interferometer based on four-wave mixing (FWM), achieving a 4 dB SNR enhancement and a sensitivity 1.6 times beyond the SQL [112]. Subsequent innovations, such as replacing the second nonlinear interaction with balanced homodyne detection (BHD), demonstrated remarkable resilience to optical loss, maintaining sensitivities exceeding the SQL by 4 dB even with 35% loss [113]. Practical implementations extend to fiber-based systems, where Liu et al. utilized amplitude-squeezed light within a fiber Mach–Zehnder interferometer to enhance low-frequency phase measurements by 2 dB [32]. Recent progress includes compact interferometers combining multiple OPAs, achieving sensitivities approaching the Heisenberg limit [105], and investigations into broadband squeezed light for suppressing vacuum noise across wider spectral ranges, highlighting the importance of tolerance to detection inefficiency and detuning [114,115]. In interferometry, squeezed inputs enhance FI by up to 6 dB in SU(1,1) configurations, yielding input/output gains that improve phase sensitivity beyond SQL, even in lossy channels where Holevo bounds indicate 20∼30% less information degradation compared to classical light [100,116].

4.2. Gravitational Wave Detection

Large-scale interferometers like LIGO represent a paramount application where squeezed light has transitioned from proof of principle to operational technology, directly impacting astrophysical discovery. The fundamental Michelson interferometer design [117–119] saw its first quantum-enhanced sensitivity improvement (44%) through squeezed vacuum injection demonstrated by Goda et al. in 2008 [93]. This paved the way for the integration of squeezed light into advanced gravitational wave observatories. The application of frequency-dependent squeezing, particularly at low frequencies (∼150 Hz), is crucial for detecting specific classes of astrophysical events [33]. Successful deployments in GEO600 and Virgo observatories, employing vacuum squeezing, expanded their observational range by a factor of 2 dB within the 3.7∼4.0 kHz band [107]. Advanced LIGO and Virgo now routinely employ quadrature-phase-squeezed states to enhance detection sensitivity across broad frequency bands, marking a milestone in applying quantum metrology to macroscopic observatories [34,97]. Recent demonstrations achieving up to 6 dB of quantum noise reduction underscore the ongoing potential for significant sensitivity gains in kilometer-scale detectors [120]. Table 1 summarizes key achievements in gravitational wave detection using squeezed light.

Table 1. Summary of sensitivity enhancements in gravitational wave detection using squeezed light.

Year	Institution	Squeezing Degree of Light (dB)	Noise Suppression	Reference
2008	LIGO	9.3 ± 0.1	44% improvement	[93]
2011	GEO 600	10	3.5 dB	[41]
2013	Advanced LIGO	10.3 ± 0.2	2.15 dB	[33]
2013	GEO 600	10	2.0 dB within 11 months	[107]
2019	Virgo	10	3.2 ± 0.1 dB	[97]
2019	LIGO O3	7.3 ± 0.3	2.7 ± 0.1 dB	[34]
2020	Advanced Virgo	12.0	$5 \sim 8$ dB	[121]
2021	GEO 600	10	6.03 ± 0.02 dB	[120]
2023	LIGO O4	$16.9 \sim 17$	$4.0 \sim 5.8$ dB	[94]
2024	LIGO	17.4	3 dB	[122]

4.3. Magnetometry

Quantum magnetometers, surpassing traditional fluxgate devices [123–125], face fundamental limits imposed by atomic spin projection noise (SPN) and photon shot noise (PSN) once classical noise sources are suppressed [126–128]. Squeezed light offers a pathway to overcome these quantum limits. Initial theoretical analyses by Kupriyanov et al. suggested squeezed light could enhance sensitivity in optically pumped magnetometers (OPMs) operating in phase-sensitive modes [129]. Petersen et al. later demonstrated theoretically that finite-bandwidth squeezed probe light could improve magnetic field variance estimates [130]. Experimental validation followed, as demonstrated in Table 1. Wolfgramm et al. achieved a 3.2 dB noise reduction below the SQL in Faraday rotation measurements using polarization-squeezed light at the Rb D1 line, corresponding to a sensitivity of 4.6×10^{-8} T/Hz$^{1/2}$ [27]. Horrom et al. developed an all-optical quantum-enhanced magnetometer using two atomic cells, observing ∼2 dB of noise reduction across a wide bandwidth (100 Hz to MHz) and identifying an optimal atomic density regime below which squeezing provides a clear advantage, potentially hindered at higher densities by atomic absorption and back-action noise amplification [29]. Otterstrom et al. demonstrated a compact, single-cell approach utilizing FWM to generate two-mode intensity-difference squeezing intrinsically linked to nonlinear magneto-optical rotation (NMOR), achieving 4.7 dB of quantum noise reduction and improving sensitivity from 33.2 pT/Hz$^{1/2}$ to

19.3 pT/Hz$^{1/2}$ [131]. Subsequent work explored the interplay between squeezing and noise in amplitude-modulated NMOR, confirming a 15% quantum enhancement despite overall sensitivity trade-offs [132,133]. Microcavity optomechanical magnetometers have also benefited, with Li et al. showing a 20% sensitivity improvement (peak sensitivity 30 pT/Hz$^{1/2}$) using phase-squeezed light to suppress PSN [134]. A significant advancement by Troullinou et al. involved applying polarization-squeezed light to a Bell–Bloom magnetometer, achieving back-action evasion by shunting associated anti-squeezed noise into an unmeasured spin component. This resulted in a 17% quantum enhancement (500 fT/Hz$^{1/2}$) and demonstrated the potential for sub-pT/Hz$^{1/2}$ sensitivities, later optimized further by density tuning [30,135,136]. Studies also indicate that self-generated squeezing during magnetic sensing may not always be beneficial, with optimal sensitivity sometimes occurring at probe powers below the squeezing threshold [137]. Recent approaches combine spin-squeezed atomic ensembles (Bose–Einstein condensates) with externally generated resonant squeezed light, achieving high sensitivities (6.2 pT/Hz$^{1/2}$) in compact areas [138]. Squeezed light also enhances spin noise spectroscopy, improving the SNR of Faraday rotation-based spin noise spectra by up to 2.6 dB [139,140] and boosting the sensitivity of single-beam magnetometers from 28.3 pT/Hz$^{1/2}$ to 19.5 pT/Hz$^{1/2}$ [141]. Furthermore, Wu et al. demonstrated a quantum gradiometer using entangled twin beams within an NMOR scheme, suppressing common-mode magnetic noise and PSN to achieve an impressive gradient sensitivity of 18 fT/cm/Hz$^{1/2}$ in noisy environments, with a 5.5 dB PSN reduction at 20 Hz [142]. Table 2 summarizes key achievements in magnetic field measurement using squeezed light.

Table 2. Summary of magnetic field measurement sensitivity using squeezed light.

Year	Institution	Squeezing Degree of Light (dB)	Noise Suppression (Sensitivity) *	Reference
2010	ICFO (Spain)	3.6	32 pT/Hz$^{1/2}$	[27]
2012	College of William and Mary (USA)	2.0 ± 0.35	2 pT/Hz$^{1/2}$	[29]
2014	Brigham Young University (USA)	4.5 ± 0.1	19.3 pT/Hz$^{1/2}$	[131]
2015	College of William and Mary (USA)	$3.5 \sim 4$	2 dB	[132]
2018	University of Queensland (Australia)	2.2	29.2 nT/Hz$^{1/2}$	[134]
2021	ICFO (Spain)	1.9	500 fT/Hz$^{1/2}$	[30]
2021	Shanxi University (China)	4.0 ± 0.3	19.5 pT/Hz$^{1/2}$	[141]
2021	Gakushuin University (Japan)	–	6.2 pT/Hz$^{1/2}$	[138]
2021	Fudan University (China)	1.9	$>$ 200 fT/Hz$^{1/2}$	[137]
2022	College of William and Mary (USA)	2.0	$>$ 250 pT/Hz$^{1/2}$	[133]
2023	Shanghai Jiao Tong University (China)	7.0	18 fT/cm/Hz$^{1/2}$	[142]
2025	Ariel University (Israel)	3.5	1 pT/Hz$^{1/2}$	[143]

* Sensitivity units are given in tesla per square root hertz (T/Hz$^{1/2}$), with prefixes: n = nano (10^{-9}), p = pico (10^{-12}), f = femto (10^{-15}).

4.4. Biomedical Sensing

Squeezed light is emerging as a powerful tool for enhancing optical microscopy and spectroscopy in life sciences [144]. By replacing classical light with quadrature-amplitude-squeezed states, the sensitivity of techniques like laser microimaging can be substantially improved, providing higher signal-to-noise ratios (SNRs) at lower photon fluxes, thus mitigating photodamage [96]. This is particularly impactful for stimulated Raman scattering (SRS) microscopy. Both continuous-wave and femtosecond-pulsed squeezed light have been employed to enhance the SNR of SRS signals [145,146]. Casacio et al. provided a critical benchmark, demonstrating that while classical light provides the highest SNR

at the biological damage threshold power, picosecond-pulsed amplitude-squeezed light offers a 1 dB SNR enhancement in SRS imaging of yeast cells below this threshold, enabling quantum-enhanced microscopic visualization [147]. Beyond spectroscopy, squeezed light improves spatial resolution. Taylor et al. achieved sub-diffraction-limited quantum imaging within living cells, showing a 14% resolution enhancement compared to classical resources [42]. In microrheology experiments inside yeast cells, squeezed light reduced amplitude noise by over 42% relative to the quantum noise limit [99]. Exploring quantum correlations further, Villabona-Monsalve et al. utilized entangled photon pairs to study entangled two-photon absorption (ETPA) in flavoproteins, highlighting the potential of quantum light for novel fluorescent sensing modalities [148]. Table 3 summarizes key achievements in biomedical sensing using squeezed light.

Table 3. Summary of sensitivity enhancements in biomedical sensing using squeezed light.

Year	Institution	Squeezing Degree of Light	Noise Suppression	Reference
2013	University of Queensland (Australia)	75% below SNL	42% improvement	[99]
2014	University of Queensland (Australia)	10 dB	14% enhancement	[42]
2020	Oak Ridge National Laboratory (USA)	5 dB	3 dB	[149]
2020	Technical University of Denmark (Denmark)	7 dB	3.6 dB SNR improvement	[145]
2020	University of Oxford (UK)	–	0.3 dB	[146]
2021	University of Queensland (Australia)	1.4 dB	35% SNR improvement	[147]

4.5. Force and Displacement Sensing

Optomechanical systems for force and displacement measurement are fundamentally limited by shot noise and radiation pressure noise (RPN) [106,150,151]. Squeezed light injection provides a direct route for surpassing these limits. Theoretical proposals suggest optical parametric amplification (OPA) within cavities can generate squeezed states for high-precision displacement measurement by attenuating quantum noise in specific quadratures [152]. OPA-assisted dissipative optomechanical systems offer enhanced weak force detection sensitivity [153] while also facilitating improved mechanical mode cooling, squeezing [154,155], and enhanced optomechanical coupling [156,157]. Experimentally, injecting squeezed vacuum into cold atomic ensemble optomechanical systems enables force detection below the SQL [37]. Hybrid configurations, employing squeezed light alongside quantum noise cancellation techniques, further increase force sensitivity beyond fundamental limits [158,159]. Practical demonstrations include using phase-squeezed light to improve mirror position and momentum estimation accuracy by 15% and 12%, respectively [160], and theoretical analyses quantifying the quantum Fisher information enhancement for force sensing in squeezed-vacuum-driven optomechanical systems [161]. Table 4 summarizes key achievements in force and displacement sensing using squeezed light.

Table 4. Summary of sensitivity enhancements in force and displacement sensing using squeezed light.

Year	Institution	Squeezing Degree of Light	Noise Suppression	Reference
2013	University of Colorado (USA)	32% below SNL	1.7 ± 0.2 dB	[162]
2013	University of Tokyo (Japan)	3.62 ± 0.26 dB	$3.28 \sim 3.48$ dB	[160]
2018	Aalto University (Finland)	10 dB	1.1 ± 0.4 dB	[150]
2020	Northwestern University (USA)	12 dB	0.7 ± 0.1 dB	[151]
2023	University of Arizona (USA)	4 dB	2.0 ± 0.2 dB	[157]

Table 4. *Cont.*

Year	Institution	Squeezing Degree of Light	Noise Suppression	Reference
2023	University of Arizona (USA)	10 dB	acceleration noise of 2×10^{-11} m/s^2/Hz$^{1/2}$	[38]
2024	Hunan Normal University (China)	–	3 orders enhancement	[122]
2024	University of Vienna (Australia)	5 dB	5 μrad/s	[159]

4.6. Quantum-Enhanced Radar and Ranging

Quantum radar concepts exploit entangled or squeezed light to potentially achieve target detection and ranging sensitivities beyond the SQL, approaching the Heisenberg limit ($\Delta\phi \approx 1/N$). Early theoretical work proposed combining squeezed-vacuum injection (SVI) with phase-sensitive amplification (PSA) to improve the resolution of laser detection and ranging (LADAR) systems, overcoming the limitations of balanced homodyne detection (BHD) efficiency and enhancing signal SNR, spatial resolution, and ranging accuracy [28,163]. Subsequent experimental efforts by Bi et al. utilized quantum phase-sensitive amplification based on SVI to compensate for photon loss, demonstrating a 1.71-fold resolution improvement [39]. Practical deployment faces challenges like atmospheric turbulence degrading entanglement. Masada addressed this by developing and verifying an entanglement quantification method for dual-mode squeezed light sources under loss, observing significant squeezing and anti-squeezing levels [164,165]. Theoretical analyses indicate that substantial squeezing (e.g., 8 dB) could improve the SNR of quantum LADAR by factors exceeding 6, offering higher spatial resolution [35]. Laboratory implementations of quantum two-mode squeezing (QTMS) radar using microwave-frequency entangled signals generated by Josephson parametric amplifiers (JPAs) have been realized [166], with simulations suggesting that engineered JPAs (EJPAs) could provide an additional 6 dB SNR improvement over conventional QTMS radar designs [167].

4.7. Atomic Clocks and Fundamental Physics Searches

Optical atomic clocks represent the pinnacle of quantum sensor precision, achieving frequency stabilities that do not deviate by more than one second over billions of years [168]. These devices leverage atomic transitions as frequency references and are instrumental in probing fundamental physics, including searches for new forces, tests of General Relativity foundations, dark matter detection, and gravitational wave sensing [169,170]. Squeezed light plays a critical role in enhancing these clocks by reducing quantum mechanical projection noise, which limits measurement accuracy in coherent atomic ensembles [33,171]. While entangled atoms have been used to improve stability [172], squeezing offers a complementary pathway to surpass the projection noise limit, enabling Heisenberg-limited sensitivities [173]. Recent advancements demonstrate that spin-squeezed states can entangle atoms, correlating their quantum states to minimize noise and boost clock precision [174]. For instance, hybrid quantum-classical atomic clocks utilizing weakly squeezed states have approached Heisenberg-limited performance [95]. These enhancements not only refine timekeeping but also amplify the clocks' utility in detecting subtle spacetime variations associated with dark matter or gravitational waves [175]. Entanglement-enhanced quantum metrology, as detailed in comprehensive reviews [176], underscores the synergy between squeezing and entanglement for achieving sensitivities beyond the standard quantum limit.

5. Outlook and Future Perspective

Squeezed light, a cornerstone non-classical state of the optical field, has emerged as a transformative quantum resource for advancing quantum sensing technologies. This review has synthesized key experimental methodologies for generating squeezed states

and highlighted their deployment across diverse applications—from surpassing standard quantum limits in interferometry and gravitational wave detection to achieving quantum-enhanced sensing and imaging.

While contemporary squeezed-light sources now achieve remarkable squeezing levels exceeding 12 dB and are progressing toward commercialization [177], significant challenges persist in fully harnessing their potential for sub-shot-noise sensing. Simply substituting classical coherent light sources with squeezed states rarely yields optimal performance without addressing context-specific quantum-classical noise trade-offs. This limitation is acutely evident in ultra-sensitive applications such as spin-exchange relaxation-free (SERF) magnetometers, where femtotesla-scale sensitivities [126,178] demand meticulous management of optical losses, back-action noise, and decoherence pathways. The integration of squeezed light into such systems necessitates rigorous theoretical modeling to identify operating regimes where quantum advantages outweigh inevitable compromises in signal fidelity or bandwidth.

Looking forward, the maturation of squeezed-light technologies hinges on overcoming three interconnected frontiers:

1. Loss Mitigation: Developing low-loss optical interfaces and novel materials to preserve squeezing fidelity in real-world environments;
2. Bandwidth Scalability: Engineering broadband squeezed sources compatible with dynamic sensing and high-rate quantum communication;
3. Hybrid Architectures: Combining squeezed states with discrete-variable or spin-based platforms to exploit complementary quantum advantages.

As these advances converge, squeezed light will transition from laboratory demonstrations to enabling technologies for quantum-enhanced metrology, fault-tolerant computation, and distributed quantum networks—ultimately redefining the boundaries of precision measurement and information processing [43,179,180].

Author Contributions: Conceptualization, X.H. and W.L.; investigation, X.H., L.Z. and Q.Y.; writing—original draft preparation, X.H.; writing—review and editing, K.W. and Y.Z.; visualization, X.H. and L.T.; funding acquisition, K.W. and Y.Z. All authors have read and agreed to the published version of the manuscript.

Funding: This research was funded by Wei K. of the National Science Foundation of China (NSFC) under Grants No. 62203030 and No. 61925301 for Distinguished Young Scholars, the Innovation Program for Quantum Science and Technology under Grant No. 2021ZD0300401, and the Fundamental Research Funds for the Central Universities.

Institutional Review Board Statement: Not applicable.

Informed Consent Statement: Not applicable.

Data Availability Statement: Not applicable.

Acknowledgments: During the preparation of this manuscript/study, the author(s) used DeepSeek-V3 for the purposes of language polishing. The authors have reviewed and edited the output and take full responsibility for the content of this publication.

Conflicts of Interest: The authors declare no conflicts of interest.

References

1. Pelucchi, E.; Fagas, G.; Aharonovich, I.; Englund, D.; Figueroa, E.; Gong, Q.; Hannes, H.; Liu, J.; Lu, C.Y.; Matsuda, N.; et al. The potential and global outlook of integrated photonics for quantum technologies. *Nat. Rev. Phys.* **2022**, *4*, 194–208. [CrossRef]
2. Wang, J.; Sciarrino, F.; Laing, A.; Thompson, M.G. Integrated photonic quantum technologies. *Nat. Photonics* **2020**, *14*, 273–284. [CrossRef]

3. Karnieli, A.; Rivera, N.; Arie, A.; Kaminer, I. The coherence of light is fundamentally tied to the quantum coherence of the emitting particle. *Sci. Adv.* **2021**, *7*, eabf8096. [CrossRef]
4. Krisnanda, T.; Tham, G.Y.; Paternostro, M.; Paterek, T. Observable quantum entanglement due to gravity. *Npj Quantum Inf.* **2020**, *6*, 12. [CrossRef]
5. Klauck, F.; Teuber, L.; Ornigotti, M.; Heinrich, M.; Scheel, S.; Szameit, A. Observation of PT-symmetric quantum interference. *Nat. Photonics* **2019**, *13*, 883–887. [CrossRef]
6. Guo, X.; Breum, C.R.; Borregaard, J.; Izumi, S.; Larsen, M.V.; Gehring, T.; Christandl, M.; Neergaard-Nielsen, J.S.; Andersen, U.L. Distributed quantum sensing in a continuous-variable entangled network. *Nat. Phys.* **2020**, *16*, 281–284. [CrossRef]
7. Kutas, M.; Haase, B.; Bickert, P.; Riexinger, F.; Molter, D.; von Freymann, G. Terahertz quantum sensing. *Sci. Adv.* **2020**, *6*, eaaz8065. [CrossRef]
8. Bongs, K.; Holynski, M.; Vovrosh, J.; Bouyer, P.; Condon, G.; Rasel, E.; Schubert, C.; Schleich, W.P.; Roura, A. Taking atom interferometric quantum sensors from the laboratory to real-world applications. *Nat. Rev. Phys.* **2019**, *1*, 731–739. [CrossRef]
9. Wang, X.; Su, Y.; Luo, C.; Nian, F.; Teng, L. Color image encryption algorithm based on hyperchaotic system and improved quantum revolving gate. *Multimed. Tools Appl.* **2022**, *81*, 13845–13865. [CrossRef]
10. Abobeih, M.; Randall, J.; Bradley, C.; Bartling, H.; Bakker, M.; Degen, M.; Markham, M.; Twitchen, D.; Taminiau, T. Atomic-scale imaging of a 27-nuclear-spin cluster using a quantum sensor. *Nature* **2019**, *576*, 411–415. [CrossRef] [PubMed]
11. Barry, J.F.; Turner, M.J.; Schloss, J.M.; Glenn, D.R.; Song, Y.; Lukin, M.D.; Park, H.; Walsworth, R.L. Optical magnetic detection of single-neuron action potentials using quantum defects in diamond. *Proc. Natl. Acad. Sci. USA* **2016**, *113*, 14133–14138. [CrossRef]
12. Nguyen, H.Q.; Derkach, I.; Hajomer, A.A.; Chin, H.M.; Oruganti, A.N.; Andersen, U.L.; Usenko, V.; Gehring, T. Digital reconstruction of squeezed light for quantum information processing. *Npj Quantum Inf.* **2025**, *11*, 71. [CrossRef]
13. Zhao, Y.; Aritomi, N.; Capocasa, E.; Leonardi, M.; Eisenmann, M.; Guo, Y.; Polini, E.; Tomura, A.; Arai, K.; Aso, Y.; et al. Frequency-dependent squeezed vacuum source for broadband quantum noise reduction in advanced gravitational-wave detectors. *Phys. Rev. Lett.* **2020**, *124*, 171101. [CrossRef] [PubMed]
14. Sarkar, J.; Salunkhe, K.V.; Mandal, S.; Ghatak, S.; Marchawala, A.H.; Das, I.; Watanabe, K.; Taniguchi, T.; Vijay, R.; Deshmukh, M.M. Quantum-noise-limited microwave amplification using a graphene Josephson junction. *Nat. Nanotechnol.* **2022**, *17*, 1147–1152. [CrossRef]
15. Auzinsh, M.; Budker, D.; Kimball, D.; Rochester, S.; Stalnaker, J.; Sushkov, A.; Yashchuk, V. Can a Quantum Nondemolition Measurement Improve the Sensitivity of an Atomic Magnetometer? *Phys. Rev. Lett.* **2004**, *93*, 173002. [CrossRef]
16. Pecoraro, A.; Cardano, F.; Marrucci, L.; Porzio, A. Continuous-variable entangled states of light carrying orbital angular momentum. *Phys. Rev. A* **2019**, *100*, 012321. [CrossRef]
17. Mehmet, M.; Vahlbruch, H. The squeezed light source for the Advanced Virgo detector in the observation run O3. *Galaxies* **2020**, *8*, 79. [CrossRef]
18. Gao, T.; von Helversen, M.; Antón-Solanas, C.; Schneider, C.; Heindel, T. Atomically-thin single-photon sources for quantum communication. *Npj 2D Mater. Appl.* **2023**, *7*, 4. [CrossRef]
19. Lewenstein, M.; Ciappina, M.F.; Pisanty, E.; Rivera-Dean, J.; Stammer, P.; Lamprou, T.; Tzallas, P. Generation of optical Schrödinger cat states in intense laser–matter interactions. *Nat. Phys.* **2021**, *17*, 1104–1108. [CrossRef]
20. Qi, S.F.; Jing, J. Generating NOON states in circuit QED using a multiphoton resonance in the presence of counter-rotating interactions. *Phys. Rev. A* **2020**, *101*, 033809. [CrossRef]
21. Ge, W.; Sawyer, B.C.; Britton, J.W.; Jacobs, K.; Bollinger, J.J.; Foss-Feig, M. Trapped ion quantum information processing with squeezed phonons. *Phys. Rev. Lett.* **2019**, *122*, 030501. [CrossRef]
22. Korkmaz, U.; Türkpençe, D. Transfer of quantum information via a dissipative protocol for data classification. *Phys. Lett. A* **2022**, *426*, 127887. [CrossRef]
23. Tan, H.; Li, J. Einstein-Podolsky-Rosen entanglement and asymmetric steering between distant macroscopic mechanical and magnonic systems. *Phys. Rev. Res.* **2021**, *3*, 013192. [CrossRef]
24. Mohamed, A.B.A.; Rahman, A.U.; Eleuch, H. Temporal quantum memory and non-locality of two trapped ions under the effect of the intrinsic decoherence: Entropic uncertainty, trace norm nonlocality and entanglement. *Symmetry* **2022**, *14*, 648. [CrossRef]
25. Baccari, F.; Augusiak, R.; Šupić, I.; Tura, J.; Acín, A. Scalable bell inequalities for qubit graph states and robust self-testing. *Phys. Rev. Lett.* **2020**, *124*, 020402. [CrossRef] [PubMed]
26. Eberle, T.; Steinlechner, S.; Bauchrowitz, J.; Händchen, V.; Vahlbruch, H.; Mehmet, M.; Müller-Ebhardt, H.; Schnabel, R. Quantum Enhancement of the Zero-Area Sagnac Interferometer Topology for Gravitational Wave Detection. *Phys. Rev. Lett.* **2010**, *104*, 251102. [CrossRef] [PubMed]
27. Wolfgramm, F.; Cere, A.; Beduini, F.A.; Predojević, A.; Koschorreck, M.; Mitchell, M.W. Squeezed-light optical magnetometry. *Phys. Rev. Lett.* **2010**, *105*, 053601. [CrossRef]
28. Dutton, Z.; Shapiro, J.H.; Guha, S. LADAR resolution improvement using receivers enhanced with squeezed-vacuum injection and phase-sensitive amplification. *J. Opt. Soc. Am. B* **2010**, *27*, A63–A72. [CrossRef]

29. Horrom, T.; Singh, R.; Dowling, J.P.; Mikhailov, E.E. Quantum-enhanced magnetometer with low-frequency squeezing. *Phys. Rev. A—Atomic Mol. Opt. Phys.* **2012**, *86*, 023803. [CrossRef]
30. Troullinou, C.; Jiménez-Martínez, R.; Kong, J.; Lucivero, V.; Mitchell, M. Squeezed-light enhancement and backaction evasion in a high sensitivity optically pumped magnetometer. *Phys. Rev. Lett.* **2021**, *127*, 193601. [CrossRef]
31. Li, D.; Yuan, C.H.; Ou, Z.; Zhang, W. The phase sensitivity of an SU (1, 1) interferometer with coherent and squeezed-vacuum light. *New J. Phys.* **2014**, *16*, 073020. [CrossRef]
32. Liu, F.; Zhou, Y.; Yu, J.; Guo, J.; Wu, Y.; Xiao, S.; Wei, D.; Zhang, Y.; Jia, X.; Xiao, M. Squeezing-enhanced fiber Mach-Zehnder interferometer for low-frequency phase measurement. *Appl. Phys. Lett.* **2017**, *110*, 021106 . [CrossRef]
33. Aasi, J.; Abadie, J.; Abbott, B.; Abbott, R.; Abbott, T.; Abernathy, M.; Adams, C.; Adams, T.; Addesso, P.; Adhikari, R.; et al. Enhanced sensitivity of the LIGO gravitational wave detector by using squeezed states of light. *Nat. Photonics* **2013**, *7*, 613–619. [CrossRef]
34. Tse, M.; Yu, H.; Kijbunchoo, N.; Fernandez-Galiana, A.; Dupej, P.; Barsotti, L.; Blair, C.; Brown, D.; Dwyer, S.e.; Effler, A.; et al. Quantum-enhanced advanced LIGO detectors in the era of gravitational-wave astronomy. *Phys. Rev. Lett.* **2019**, *123*, 231107. [CrossRef] [PubMed]
35. Feng, F.; Xu, J.M.; Ma, J.T.; Liu, Z.L.; Zhang, W.J. Quantum Lidar Based on Squeezed Sates of Light. *Acta Photonica SINICA* **2017**, *46* , 195–203.
36. Wang, H.; Qin, J.; Ding, X.; Chen, M.C.; Chen, S.; You, X.; He, Y.M.; Jiang, X.; You, L.; Wang, Z.; et al. Boson sampling with 20 input photons and a 60-mode interferometer in a 1 0 14-dimensional hilbert space. *Phys. Rev. Lett.* **2019**, *123*, 250503. [CrossRef]
37. Motazedifard, A.; Bemani, F.; Naderi, M.; Roknizadeh, R.; Vitali, D. Force sensing based on coherent quantum noise cancellation in a hybrid optomechanical cavity with squeezed-vacuum injection. *New J. Phys.* **2016**, *18*, 073040. [CrossRef]
38. Brady, A.J.; Chen, X.; Xia, Y.; Manley, J.; Dey Chowdhury, M.; Xiao, K.; Liu, Z.; Harnik, R.; Wilson, D.J.; Zhang, Z.; et al. Entanglement-enhanced optomechanical sensor array with application to dark matter searches. *Commun. Phys.* **2023**, *6*, 237. [CrossRef]
39. Bi, S.; Zhu, H.; Du, J.; Zhou, Z.; Chen, H.; Shen, M.; Zhang, S.; Sheng, Z. Realization of quantum lidar imaging system. In Proceedings of the Infrared Remote Sensing and Instrumentation XXVIII, Online, 24 August–4 September 2020; SPIE: Philadelphia, PA, USA, 2020; Volume 11502, pp. 10–15.
40. Wu, M.C.; Brewer, N.R.; Speirs, R.W.; Jones, K.M.; Lett, P.D. Two-beam coupling in the production of quantum correlated images by four-wave mixing. *Opt. Express* **2021**, *29*, 16665–16675. [CrossRef]
41. Collaboration, T.L.S. A gravitational wave observatory operating beyond the quantum shot-noise limit. *Nat. Phys.* **2011**, *7*, 962–965. [CrossRef]
42. Taylor, M.A.; Janousek, J.; Daria, V.; Knittel, J.; Hage, B.; Bachor, H.A.; Bowen, W.P. Subdiffraction-limited quantum imaging within a living cell. *Phys. Rev. X* **2014**, *4*, 011017. [CrossRef]
43. Patra, A.; Gupta, R.; Roy, S.; Das, T.; Sen, A. Quantum dense coding network using multimode squeezed states of light. *Phys. Rev. A* **2022**, *106*, 052607. [CrossRef]
44. Ou, Z. Enhancement of the phase-measurement sensitivity beyond the standard quantum limit by a nonlinear interferometer. *Phys. Rev. A—Atomic Mol. Opt. Phys.* **2012**, *85*, 023815. [CrossRef]
45. Park, T.; Stokowski, H.; Ansari, V.; Gyger, S.; Multani, K.K.; Celik, O.T.; Hwang, A.Y.; Dean, D.J.; Mayor, F.; McKenna, T.P.; et al. Single-mode squeezed-light generation and tomography with an integrated optical parametric oscillator. *Sci. Adv.* **2024**, *10*, eadl1814. [CrossRef]
46. Wasilewski, W.; Fernholz, T.; Jensen, K.; Madsen, L.; Krauter, H.; Muschik, C.; Polzik, E. Generation of two-mode squeezed and entangled light in a single temporal and spatial mode. *Opt. Express* **2009**, *17*, 14444–14457. [CrossRef] [PubMed]
47. Cardoso, F.R.; Rossatto, D.Z.; Fernandes, G.P.; Higgins, G.; Villas-Boas, C.J. Superposition of two-mode squeezed states for quantum information processing and quantum sensing. *Phys. Rev. A* **2021**, *103*, 062405. [CrossRef]
48. Roman-Rodriguez, V.; Fainsin, D.; Zanin, G.L.; Treps, N.; Diamanti, E.; Parigi, V. Multimode squeezed state for reconfigurable quantum networks at telecommunication wavelengths. *Phys. Rev. Res.* **2024**, *6*, 043113. [CrossRef]
49. Kopylov, D.A.; Meier, T.; Sharapova, P.R. Theory of multimode squeezed light generation in lossy media. *Quantum* **2025**, *9*, 1621. [CrossRef]
50. Lee, C.W.; Lee, J.H.; Seok, H. Squeezed-light-driven force detection with an optomechanical cavity in a Mach–Zehnder interferometer. *Sci. Rep.* **2020**, *10*, 17496. [CrossRef]
51. Gatto, D.; Facchi, P.; Tamma, V. Heisenberg-limited estimation robust to photon losses in a Mach-Zehnder network with squeezed light. *Phys. Rev. A* **2022**, *105*, 012607. [CrossRef]
52. Feng, F.; Bi, S.W.; Lu, B.Z.; Kang, M.H. Long-term stable bright amplitude-squeezed state of light at 1064 nm for quantum imaging. *Optik* **2013**, *124*, 1070–1073. [CrossRef]
53. Brida, G.; Genovese, M.; Ruo Berchera, I. Experimental realization of sub-shot-noise quantum imaging. *Nat. Photonics* **2010**, *4*, 227–230. [CrossRef]

54. Michel, T.; Haw, J.Y.; Marangon, D.G.; Thearle, O.; Vallone, G.; Villoresi, P.; Lam, P.K.; Assad, S.M. Real-time source-independent quantum random-number generator with squeezed states. *Phys. Rev. Appl.* **2019**, *12*, 034017. [CrossRef]
55. Matekole, E.S.; Cuozzo, S.L.; Prajapati, N.; Bhusal, N.; Lee, H.; Novikova, I.; Mikhailov, E.E.; Dowling, J.P.; Cohen, L. Quantum-limited squeezed light detection with a camera. *Phys. Rev. Lett.* **2020**, *125*, 113602. [CrossRef]
56. Gorlach, A.; Karnieli, A.; Dahan, R.; Cohen, E.; Pe'er, A.; Kaminer, I. Ultrafast non-destructive measurement of the quantum state of light with free electrons. In Proceedings of the CLEO: QELS_Fundamental Science, San Jose, CA, USA, 9–14 May 2021; Optica Publishing Group: Washington, DC, USA, 2021; p. FF2I–4 .
57. Matsko, A.; Novikova, I.; Welch, G.R.; Budker, D.; Kimball, D.; Rochester, S. Vacuum squeezing in atomic media via self-rotation. *Phys. Rev. A* **2002**, *66*, 043815. [CrossRef]
58. Barreiro, S.; Valente, P.; Failache, H.; Lezama, A. Polarization squeezing of light by single passage through an atomic vapor. *Phys. Rev. A—Atomic Mol. Opt. Phys.* **2011**, *84*, 033851. [CrossRef]
59. Agha, I.H.; Messin, G.; Grangier, P. Generation of pulsed and continuous-wave squeezed light with 87Rb vapor. *Opt. Express* **2010**, *18*, 4198–4205. [CrossRef] [PubMed]
60. Xu, A.; Liao, J.; Bao, G.; Wu, Y.; Chen, L. Pulsed squeezed light via self-rotation. *Opt. Commun.* **2019**, *452*, 506–509. [CrossRef]
61. Yu, Z.; Liu, S.; Guo, J.; Bao, G.; Wu, Y.; Chen, L. Enhancing vacuum squeezing via magnetic field optimization. *Opt. Express* **2022**, *30*, 17106–17114. [CrossRef] [PubMed]
62. Slusher, R.; Hollberg, L.; Yurke, B.; Mertz, J.; Valley, J. Observation of squeezed states generated by four-wave mixing in an optical cavity. *Phys. Rev. Lett.* **1985**, *55*, 2409. [CrossRef]
63. McCormick, C.; Boyer, V.; Arimondo, E.; Lett, P. Strong relative intensity squeezing by four-wave mixing in rubidium vapor. *Opt. Lett.* **2006**, *32*, 178–180. [CrossRef]
64. McCormick, C.; Marino, A.M.; Boyer, V.; Lett, P.D. Strong low-frequency quantum correlations from a four-wave-mixing amplifier. *Phys. Rev. A—Atomic Mol. Opt. Phys.* **2008**, *78*, 043816. [CrossRef]
65. Wu, M.C.; Schmittberger, B.L.; Brewer, N.R.; Speirs, R.W.; Jones, K.M.; Lett, P.D. Twin-beam intensity-difference squeezing below 10 Hz. *Opt. Express* **2019**, *27*, 4769–4780. [CrossRef]
66. Glorieux, Q.; Guidoni, L.; Guibal, S.; Likforman, J.P.; Coudreau, T. Quantum correlations by four-wave mixing in an atomic vapor in a nonamplifying regime: Quantum beam splitter for photons. *Phys. Rev. A—Atomic Mol. Opt. Phys.* **2011**, *84*, 053826. [CrossRef]
67. De Araujo, L.E.; Zhou, Z.; DiMario, M.; Anderson, B.; Zhao, J.; Jones, K.M.; Lett, P.D. Characterizing two-mode-squeezed light from four-wave mixing in rubidium vapor for quantum sensing and information processing. *Opt. Express* **2024**, *32*, 1305–1313. [CrossRef]
68. Heng, X.; Wang, W.; Wang, F.; Liu, W.; Xia, M.; Zhai, Y.; Wei, K. Enhanced multi-mode squeezing via a balanced regime in dual-four-wave mixing. *Phys. Scr.* **2025**, *100*, 035112. [CrossRef]
69. Kim, S.; Marino, A.M. Generation of 87Rb resonant bright two-mode squeezed light with four-wave mixing. *Opt. Express* **2018**, *26*, 33366–33375. [CrossRef] [PubMed]
70. Sim, G.; Kim, H.; Moon, H.S. Intensity-difference squeezing from four-wave mixing in hot 85Rb and 87Rb atoms in single diode laser pumping system. *Sci. Rep.* **2025**, *15*, 7727. [CrossRef] [PubMed]
71. Neveu, P.; Delpy, J.; Liu, S.; Banerjee, C.; Lugani, J.; Bretenaker, F.; Brion, E.; Goldfarb, F. Generation of squeezed light vacuum enabled by coherent population trapping. *Opt. Express* **2021**, *29*, 10471–10479. [CrossRef]
72. Wu, L.A.; Kimble, H.; Hall, J.; Wu, H. Generation of squeezed states by parametric down conversion. *Phys. Rev. Lett.* **1986**, *57*, 2520. [CrossRef] [PubMed]
73. Breitenbach, G.; Schiller, S.; Mlynek, J. Measurement of the quantum states of squeezed light. *Nature* **1997**, *387*, 471–475. [CrossRef]
74. Lam, P.; Ralph, T.; Buchler, B.; McClelland, D.; Bachor, H.; Gao, J. Optimization and transfer of vacuum squeezing from an optical parametric oscillator. *J. Opt. B Quantum Semiclassical Opt.* **1999**, *1*, 469. [CrossRef]
75. Takeno, Y.; Yukawa, M.; Yonezawa, H.; Furusawa, A. Observation of-9 dB quadrature squeezing with improvement of phase stability in homodyne measurement. *Opt. Express* **2007**, *15*, 4321–4327. [CrossRef]
76. Vahlbruch, H.; Mehmet, M.; Chelkowski, S.; Hage, B.; Franzen, A.; Lastzka, N.; Gossler, S.; Danzmann, K.; Schnabel, R. Observation of squeezed light with 10-dB quantum-noise reduction. *Phys. Rev. Lett.* **2008**, *100*, 033602. [CrossRef] [PubMed]
77. Li, F.; Tian, L.; Huang, T.; Dang, H.; Zhao, D.; Shi, S.; Wang, Y.; Yin, W.; Zheng, Y. Development of a low-intensity-noise laser source based on ultra-low-noise photodetectors in the sub-millihertz band. *Opt. Laser Technol.* **2025**, *192*, 113747. [CrossRef]
78. Mehmet, M.; Vahlbruch, H.; Lastzka, N.; Danzmann, K.; Schnabel, R. Observation of squeezed states with strong photon-number oscillations. *Phys. Rev. A—Atomic Mol. Opt. Phys.* **2010**, *81*, 013814. [CrossRef]
79. Vahlbruch, H.; Mehmet, M.; Danzmann, K.; Schnabel, R. Detection of 15 dB squeezed states of light and their application for the absolute calibration of photoelectric quantum efficiency. *Phys. Rev. Lett.* **2016**, *117*, 110801. [CrossRef]

80. Kawasaki, A.; Brunel, H.; Ide, R.; Suzuki, T.; Kashiwazaki, T.; Inoue, A.; Umeki, T.; Yamashima, T.; Sakaguchi, A.; Takase, K.; et al. Real-time observation of picosecond-timescale optical quantum entanglement towards ultrafast quantum information processing. *Nat. Photonics* **2025**, *19*, 271–276. [CrossRef]
81. Shajilal, B.; Thearle, O.; Tranter, A.; Lu, Y.; Huntington, E.; Assad, S.; Lam, P.K.; Janousek, J. 12.6 dB squeezed light at 1550 nm from a bow-tie cavity for long-term high duty cycle operation. *Opt. Express* **2022**, *30*, 37213–37223. [CrossRef] [PubMed]
82. Mehmet, M.; Ast, S.; Eberle, T.; Steinlechner, S.; Vahlbruch, H.; Schnabel, R. Squeezed light at 1550 nm with a quantum noise reduction of 12.3 dB. *Opt. Express* **2011**, *19*, 25763–25772. [CrossRef]
83. Schönbeck, A.; Thies, F.; Schnabel, R. 13 dB squeezed vacuum states at 1550 nm from 12 mW external pump power at 775 nm. *Opt. Lett.* **2017**, *43*, 110–113. [CrossRef]
84. Haus, H.A. Quantum noise, quantum measurement, and squeezing. *J. Opt. B Quantum Semiclassical Opt.* **2004**, *6*, S626. [CrossRef]
85. Matsko, A.B.; Rostovtsev, Y.V.; Cummins, H.Z.; Scully, M.O. Using slow light to enhance acousto-optical effects: Application to squeezed light. *Phys. Rev. Lett.* **2000**, *84*, 5752. [CrossRef]
86. Shelby, R.M.; Levenson, M.D.; Perlmutter, S.H.; DeVoe, R.G.; Walls, D.F. Broad-band parametric deamplification of quantum noise in an optical fiber. *Phys. Rev. Lett.* **1986**, *57*, 691. [CrossRef]
87. Rosenbluh, M.; Shelby, R.M. Squeezed optical solitons. *Phys. Rev. Lett.* **1991**, *66*, 153. [CrossRef]
88. Peuntinger, C.; Heim, B.; Müller, C.R.; Gabriel, C.; Marquardt, C.; Leuchs, G. Distribution of squeezed states through an atmospheric channel. *Phys. Rev. Lett.* **2014**, *113*, 060502. [CrossRef]
89. Dong, R.; Heersink, J.; Corney, J.F.; Drummond, P.D.; Andersen, U.L.; Leuchs, G. Experimental evidence for Raman-induced limits to efficient squeezing in optical fibers. *Opt. Lett.* **2008**, *33*, 116–118. [CrossRef]
90. Anashkina, E.A.; Andrianov, A.V.; Corney, J.F.; Leuchs, G. Chalcogenide fibers for Kerr squeezing. *Opt. Lett.* **2020**, *45*, 5299–5302. [CrossRef]
91. Schnabel, R. Squeezed states of light and their applications in laser interferometers. *Phys. Rep.* **2017**, *684*, 1–51. [CrossRef]
92. Caves, C.M. Quantum-mechanical noise in an interferometer. *Phys. Rev. D* **1981**, *23*, 1693. [CrossRef]
93. Goda, K.; Miyakawa, O.; Mikhailov, E.E.; Saraf, S.; Adhikari, R.; McKenzie, K.; Ward, R.; Vass, S.; Weinstein, A.J.; Mavalvala, N. A quantum-enhanced prototype gravitational-wave detector. *Nat. Phys.* **2008**, *4*, 472–476. [CrossRef]
94. Ganapathy, D.; Jia, W.; Nakano, M.; Xu, V.; Aritomi, N.; Cullen, T.; Kijbunchoo, N.; Dwyer, S.; Mullavey, A.; McCuller, L.; et al. Broadband quantum enhancement of the LIGO detectors with frequency-dependent squeezing. *Phys. Rev. X* **2023**, *13*, 041021. [CrossRef]
95. Pezzè, L.; Smerzi, A. Heisenberg-limited noisy atomic clock using a hybrid coherent and squeezed state protocol. *Phys. Rev. Lett.* **2020**, *125*, 210503. [CrossRef]
96. Lawrie, B.; Pooser, R.; Maksymovych, P. Squeezing noise in microscopy with quantum light. *Trends Chem.* **2020**, *2*, 683–686. [CrossRef]
97. Acernese, F.; Agathos, M.; Aiello, L.; Allocca, A.; Amato, A.; Ansoldi, S.; Antier, S.; Arène, M.; Arnaud, N.; Ascenzi, S.; et al. Increasing the astrophysical reach of the advanced virgo detector via the application of squeezed vacuum states of light. *Phys. Rev. Lett.* **2019**, *123*, 231108. [CrossRef]
98. Jasperse, M.; Turner, L.; Scholten, R. Relative intensity squeezing by four-wave mixing with loss: An analytic model and experimental diagnostic. *Opt. Express* **2011**, *19*, 3765–3774. [CrossRef] [PubMed]
99. Taylor, M.A.; Janousek, J.; Daria, V.; Knittel, J.; Hage, B.; Bachor, H.A.; Bowen, W.P. Biological measurement beyond the quantum limit. *Nat. Photonics* **2013**, *7*, 229–233. [CrossRef]
100. Braunstein, S.L.; Caves, C.M. Statistical distance and the geometry of quantum states. *Phys. Rev. Lett.* **1994**, *72*, 3439. [CrossRef]
101. Helstrom, C.W. Quantum detection and estimation theory. *J. Stat. Phys.* **1969**, *1*, 231–252. [CrossRef]
102. Holevo, A.S. Bounds for the quantity of information transmitted by a quantum communication channel. *Probl. Peredachi Informatsii* **1973**, *9*, 3–11.
103. Giovannetti, V.; Lloyd, S.; Maccone, L. Advances in quantum metrology. *Nat. Photonics* **2011**, *5*, 222–229. [CrossRef]
104. Demkowicz-Dobrzański, R.; Jarzyna, M.; Kołodyński, J. Quantum limits in optical interferometry. *Prog. Opt.* **2015**, *60*, 345–435.
105. Zuo, X.; Yan, Z.; Feng, Y.; Ma, J.; Jia, X.; Xie, C.; Peng, K. Quantum interferometer combining squeezing and parametric amplification. *Phys. Rev. Lett.* **2020**, *124*, 173602. [CrossRef]
106. Buchmann, L.; Schreppler, S.; Kohler, J.; Spethmann, N.; Stamper-Kurn, D. Complex squeezing and force measurement beyond the standard quantum limit. *Phys. Rev. Lett.* **2016**, *117*, 030801. [CrossRef]
107. Grote, H.; Danzmann, K.; Dooley, K.L.; Schnabel, R.; Slutsky, J.; Vahlbruch, H. First long-term application of squeezed states of light in a gravitational-wave observatory. *Phys. Rev. Lett.* **2013**, *110*, 181101. [CrossRef] [PubMed]
108. Xiao, M.; Wu, L.A.; Kimble, H.J. Precision measurement beyond the shot-noise limit. *Phys. Rev. Lett.* **1987**, *59*, 278. [CrossRef]
109. Slusher, R.E.; Grangier, P.; LaPorta, A.; Yurke, B.; Potasek, M. Pulsed squeezed light. *Phys. Rev. Lett.* **1987**, *59*, 2566. [CrossRef]
110. Boto, A.N.; Kok, P.; Abrams, D.S.; Braunstein, S.L.; Williams, C.P.; Dowling, J.P. Quantum interferometric optical lithography: Exploiting entanglement to beat the diffraction limit. *Phys. Rev. Lett.* **2000**, *85*, 2733. [CrossRef]

111. Nagata, T.; Okamoto, R.; O'brien, J.L.; Sasaki, K.; Takeuchi, S. Beating the standard quantum limit with four-entangled photons. *Science* **2007**, *316*, 726–729. [CrossRef]
112. Hudelist, F.; Kong, J.; Liu, C.; Jing, J.; Ou, Z.; Zhang, W. Quantum metrology with parametric amplifier-based photon correlation interferometers. *Nat. Commun.* **2014**, *5*, 3049. [CrossRef]
113. Anderson, B.E.; Gupta, P.; Schmittberger, B.L.; Horrom, T.; Hermann-Avigliano, C.; Jones, K.M.; Lett, P.D. Phase sensing beyond the standard quantum limit with a variation on the SU (1, 1) interferometer. *Optica* **2017**, *4*, 752–756. [CrossRef]
114. Zhang, C.; Wang, Z.; Liu, H.; Huang, N. Tolerance enhancement of inefficient detection and frequency detuning by non-perfect phase-sensitive amplification in broadband squeezing-based precision measurement. *J. Opt. Soc. Am. B* **2022**, *39*, 2657–2664. [CrossRef]
115. Malitesta, M.; Smerzi, A.; Pezze, L. Distributed quantum sensing with squeezed-vacuum light in a configurable array of Mach-Zehnder interferometers. *Phys. Rev. A* **2023**, *108*, 032621. [CrossRef]
116. Tsang, M. Quantum metrology with open dynamical systems. *New J. Phys.* **2013**, *15*, 073005. [CrossRef]
117. Hild, S. Beyond the second generation of laser-interferometric gravitational wave observatories. *Class. Quantum Gravity* **2012**, *29*, 124006. [CrossRef]
118. Dwyer, S.; Barsotti, L.; Chua, S.; Evans, M.; Factourovich, M.; Gustafson, D.; Isogai, T.; Kawabe, K.; Khalaidovski, A.; Lam, P.; et al. Squeezed quadrature fluctuations in a gravitational wave detector using squeezed light. *Opt. Express* **2013**, *21*, 19047–19060. [CrossRef] [PubMed]
119. Abbott, B.P.; Abbott, R.; Adhikari, R.; Ajith, P.; Allen, B.; Allen, G.; Amin, R.; Anderson, S.; Anderson, W.; Arain, M.; et al. LIGO: The laser interferometer gravitational-wave observatory. *Rep. Prog. Phys.* **2009**, *72*, 076901. [CrossRef]
120. Lough, J.; Schreiber, E.; Bergamin, F.; Grote, H.; Mehmet, M.; Vahlbruch, H.; Affeldt, C.; Brinkmann, M.; Bisht, A.; Kringel, V.; et al. First demonstration of 6 dB quantum noise reduction in a kilometer scale gravitational wave observatory. *Phys. Rev. Lett.* **2021**, *126*, 041102. [CrossRef]
121. Acernese, F.; Agathos, M.; Aiello, L.; Ain, A.; Allocca, A.; Amato, A.; Ansoldi, S.; Antier, S.; Arène, M.; Arnaud, N.; et al. Quantum backaction on Kg-scale mirrors: Observation of radiation pressure noise in the advanced Virgo detector. *Phys. Rev. Lett.* **2020**, *125*, 131101. [CrossRef]
122. Jia, W.; Xu, V.; Kuns, K.; Nakano, M.; Barsotti, L.; Evans, M.; Mavalvala, N.; Collaboration†, L.S.; Abbott, R.; Abouelfettouh, I.; et al. Squeezing the quantum noise of a gravitational-wave detector below the standard quantum limit. *Science* **2024**, *385*, 1318–1321. [CrossRef]
123. Janosek, M.; Butta, M.; Dressler, M.; Saunderson, E.; Novotny, D.; Fourie, C. 1-pT noise fluxgate magnetometer for geomagnetic measurements and unshielded magnetocardiography. *IEEE Trans. Instrum. Meas.* **2019**, *69*, 2552–2560. [CrossRef]
124. Guo, Q.; Hu, T.; Chen, C.; Feng, X.; Wu, Z.; Zhang, Y.; Zhang, M.; Chang, Y.; Yang, X. A high sensitivity closed-loop spin-exchange relaxation-free atomic magnetometer with broad bandwidth. *IEEE Sensors J.* **2021**, *21*, 21425–21431. [CrossRef]
125. Trabaldo, E.; Pfeiffer, C.; Andersson, E.; Chukharkin, M.; Arpaia, R.; Montemurro, D.; Kalaboukhov, A.; Winkler, D.; Lombardi, F.; Bauch, T. SQUID magnetometer based on Grooved Dayem nanobridges and a flux transformer. *IEEE Trans. Appl. Supercond.* **2020**, *30*, 1–4. [CrossRef]
126. Heng, X.; Wei, K.; Zhao, T.; Xu, Z.; Cao, Q.; Huang, X.; Zhai, Y.; Ye, M.; Quan, W. Ultrasensitive optical rotation detection with closed-loop suppression of spin polarization error. *IEEE Trans. Instrum. Meas.* **2023**, *72*, 1501012. [CrossRef]
127. Xu, Z.; Liu, C.; Wei, K.; Gong, D.; Heng, X.; Huang, X.; Gong, D.; Wang, F.; Wang, W.; Zhai, Y.; et al. Quantification and suppression of optical non-orthogonality and light intensity noise in all-optical hot atomic sensing systems. *Opt. Laser Technol.* **2024**, *174*, 110554. [CrossRef]
128. Heng, X.; Huang, X.; Wang, W.; Wang, F.; Gong, D.; Liu, C.; Tian, G.; Zheng, J.; Zhai, Y.; Wei, K. Shot-noise-limited optical polarimetry with spin-alignment and magnetism decoupling. *Results Phys.* **2024**, *65*, 107960. [CrossRef]
129. Kupriyanov, D.; Sokolov, I. Optical detection of magnetic resonance by classical and squeezed light. *Quantum Opt. J. Eur. Opt. Soc. Part B* **1992**, *4*, 55. [CrossRef]
130. Petersen, V.; Madsen, L.B.; Mølmer, K. Gaussian-state description of squeezed light. *Phys. Rev. A—Atomic Mol. Opt. Phys.* **2005**, *72*, 053812. [CrossRef]
131. Otterstrom, N.; Pooser, R.; Lawrie, B.J. Nonlinear optical magnetometry with accessible in situ optical squeezing. *Opt. Lett.* **2014**, *39*, 6533–6536. [CrossRef]
132. Novikova, I.; Mikhailov, E.E.; Xiao, Y. Excess optical quantum noise in atomic sensors. *Phys. Rev. A* **2015**, *91*, 051804. [CrossRef]
133. Li, J.; Novikova, I. Improving sensitivity of an amplitude-modulated magneto-optical atomic magnetometer using squeezed light. *J. Opt. Soc. Am. B* **2022**, *39*, 2998–3003. [CrossRef]
134. Li, B.B.; Bílek, J.; Hoff, U.B.; Madsen, L.S.; Forstner, S.; Prakash, V.; Schäfermeier, C.; Gehring, T.; Bowen, W.P.; Andersen, U.L. Quantum enhanced optomechanical magnetometry. *Optica* **2018**, *5*, 850–856. [CrossRef]
135. Troullinou, C.; Lucivero, V.G.; Mitchell, M.W. Quantum-enhanced magnetometry at optimal number density. *Phys. Rev. Lett.* **2023**, *131*, 133602. [CrossRef]

136. Sierant, A.; Méndez-Avalos, D.; Giraldo, S.T.; Mitchell, M.W. Quantum noise in a squeezed-light-enhanced multiparameter quantum sensor. *arXiv* **2025**, arXiv:2506.08190.
137. Zhang, X.; Jin, S.; Qu, W.; Xiao, Y. Dichroism and birefringence optical atomic magnetometer with or without self-generated light squeezing. *Appl. Phys. Lett.* **2021**, *119*, 054001. [CrossRef]
138. Shibata, K.; Sekiguchi, N.; Torii, A.; Takai, J.; Hirano, T. Precise magnetometry with a spin squeezed ultracold gas and squeezed light. In Proceedings of the JSAP Annual Meetings Extended Abstracts the 82nd JSAP Autumn Meeting, Online, 10–13 September 2021; The Japan Society of Applied Physics: Tokyo, Japan, 2021; p. 1206.
139. Lucivero, V.G.; Jiménez-Martínez, R.; Kong, J.; Mitchell, M.W. Squeezed-light spin noise spectroscopy. *Phys. Rev. A* **2016**, *93*, 053802. [CrossRef]
140. Bai, L.; Zhang, L.; Yang, Y.; Chang, R.; Qin, Y.; He, J.; Wen, X.; Wang, J. Enhancement of spin noise spectroscopy of rubidium atomic ensemble by using the polarization squeezed light. *Opt. Express* **2022**, *30*, 1925–1935. [CrossRef]
141. Bai, L.; Wen, X.; Yang, Y.; Zhang, L.; He, J.; Wang, Y.; Wang, J. Quantum-enhanced rubidium atomic magnetometer based on Faraday rotation via 795 nm stokes operator squeezed light. *J. Opt.* **2021**, *23*, 085202. [CrossRef]
142. Wu, S.; Bao, G.; Guo, J.; Chen, J.; Du, W.; Shi, M.; Yang, P.; Chen, L.; Zhang, W. Quantum magnetic gradiometer with entangled twin light beams. *Sci. Adv.* **2023**, *9*, eadg1760. [CrossRef]
143. Monsa, S.; Chasid, Y.; Shuldiner, M.; Sternklar, S.; Talker, E. Vacuum squeezing enhanced micrometer scale vapor cell magnetometer. *arXiv* **2025**, arXiv:2507.07672. [CrossRef]
144. Kim, S.; Yoon, J.; Ko, G.; Kang, I.; Tian, H.; Fan, L.Z.; Li, Y.; Xiao, G.; Zhang, Q.; Cohen, A.E.; et al. Optical segmentation-based compressed readout of neuronal voltage dynamics. *Nat. Commun.* **2025**, *16*, 7194. [CrossRef]
145. de Andrade, R.B.; Kerdoncuff, H.; Berg-Sørensen, K.; Gehring, T.; Lassen, M.; Andersen, U.L. Quantum-enhanced continuous-wave stimulated Raman scattering spectroscopy. *Optica* **2020**, *7*, 470–475. [CrossRef]
146. Triginer Garces, G.; Chrzanowski, H.M.; Daryanoosh, S.; Thiel, V.; Marchant, A.L.; Patel, R.B.; Humphreys, P.C.; Datta, A.; Walmsley, I.A. Quantum-enhanced stimulated emission detection for label-free microscopy. *Appl. Phys. Lett.* **2020**, *117*, 024002. [CrossRef]
147. Casacio, C.A.; Madsen, L.S.; Terrasson, A.; Waleed, M.; Barnscheidt, K.; Hage, B.; Taylor, M.A.; Bowen, W.P. Quantum-enhanced nonlinear microscopy. *Nature* **2021**, *594*, 201–206. [CrossRef]
148. Villabona-Monsalve, J.P.; Varnavski, O.; Palfey, B.A.; Goodson III, T. Two-photon excitation of flavins and flavoproteins with classical and quantum light. *J. Am. Chem. Soc.* **2018**, *140*, 14562–14566. [CrossRef]
149. Pooser, R.; Savino, N.; Batson, E.; Beckey, J.; Garcia, J.; Lawrie, B. Truncated nonlinear interferometry for quantum-enhanced atomic force microscopy. *Phys. Rev. Lett.* **2020**, *124*, 230504. [CrossRef]
150. Ockeloen-Korppi, C.; Damskägg, E.; Paraoanu, G.S.; Massel, F.; Sillanpää, M. Revealing hidden quantum correlations in an electromechanical measurement. *Phys. Rev. Lett.* **2018**, *121*, 243601. [CrossRef]
151. Aggarwal, N.; Cullen, T.J.; Cripe, J.; Cole, G.D.; Lanza, R.; Libson, A.; Follman, D.; Heu, P.; Corbitt, T.; Mavalvala, N. Room-temperature optomechanical squeezing. *Nat. Phys.* **2020**, *16*, 784–788. [CrossRef]
152. Peano, V.; Schwefel, H.; Marquardt, C.; Marquardt, F. Intracavity squeezing can enhance quantum-limited optomechanical position detection through deamplification. *Phys. Rev. Lett.* **2015**, *115*, 243603. [CrossRef]
153. Huang, S.; Agarwal, G. Robust force sensing for a free particle in a dissipative optomechanical system with a parametric amplifier. *Phys. Rev. A* **2017**, *95*, 023844. [CrossRef]
154. Huang, S.; Chen, A. Improving the cooling of a mechanical oscillator in a dissipative optomechanical system with an optical parametric amplifier. *Phys. Rev. A* **2018**, *98*, 063818. [CrossRef]
155. Agarwal, G.; Huang, S. Strong mechanical squeezing and its detection. *Phys. Rev. A* **2016**, *93*, 043844. [CrossRef]
156. Zhang, J.S.; Li, M.C.; Chen, A.X. Enhancing quadratic optomechanical coupling via a nonlinear medium and lasers. *Phys. Rev. A* **2019**, *99*, 013843. [CrossRef]
157. Xia, Y.; Agrawal, A.R.; Pluchar, C.M.; Brady, A.J.; Liu, Z.; Zhuang, Q.; Wilson, D.J.; Zhang, Z. Entanglement-enhanced optomechanical sensing. *Nat. Photonics* **2023**, *17*, 470–477. [CrossRef]
158. Subhash, S.; Das, S.; Dey, T.N.; Li, Y.; Davuluri, S. Enhancing the force sensitivity of a squeezed light optomechanical interferometer. *Opt. Express* **2022**, *31*, 177–191. [CrossRef]
159. Silvestri, R.; Yu, H.; Stroemberg, T.; Hilweg, C.; Peterson, R.W.; Walther, P. Experimental observation of earth's rotation with quantum entanglement. *Sci. Adv.* **2024**, *10*, eado0215. [CrossRef]
160. Iwasawa, K.; Makino, K.; Yonezawa, H.; Tsang, M.; Davidovic, A.; Huntington, E.; Furusawa, A. Quantum-limited mirror-motion estimation. *Phys. Rev. Lett.* **2013**, *111*, 163602. [CrossRef]
161. Lee, C.W.; Lee, J.H.; Joo, J.; Seok, H. Quantum fisher information of an optomechanical force sensor driven by a squeezed vacuum field. *Opt. Express* **2022**, *30*, 25249–25261. [CrossRef]
162. Purdy, T.P.; Yu, P.L.; Peterson, R.W.; Kampel, N.S.; Regal, C.A. Strong optomechanical squeezing of light. *Phys. Rev. X* **2013**, *3*, 031012. [CrossRef]

163. Nair, R.; Yen, B.J.; Shapiro, J.H.; Chen, J.; Dutton, Z.; Guha, S.; da Silva, M.P. Quantum-enhanced ladar ranging with squeezed-vacuum injection, phase-sensitive amplification, and slow photodetectors. In Proceedings of the Quantum Communications and Quantum Imaging IX, San Diego, CA, USA, 21–25 August 2011; SPIE: Philadelphia, PA, USA, 2011; Volume 8163, pp. 203–216.
164. Masada, G. Two-mode squeezed light source for quantum illumination and quantum imaging II. In Proceedings of the Quantum Communications and Quantum Imaging XIV, San Diego, CA, USA, 28 August–1 September 2016; SPIE: Philadelphia, PA, USA, 2016; Volume 9980, pp. 142–152.
165. Masada, G. Verification of quantum entanglement of two-mode squeezed light source towards quantum radar and imaging. In Proceedings of the Quantum Communications and Quantum Imaging XV, San Diego, CA, USA, 6–10 August 2017; SPIE: Philadelphia, PA, USA, 2017; Volume 10409, pp. 92–97.
166. Luong, D.; Chang, C.S.; Vadiraj, A.; Damini, A.; Wilson, C.M.; Balaji, B. Receiver operating characteristics for a prototype quantum two-mode squeezing radar. *IEEE Trans. Aerosp. Electron. Syst.* **2019**, *56*, 2041–2060. [CrossRef]
167. Norouzi, M.; Hosseiny, S.M.; Seyed-Yazdi, J.; Ghamat, M.H. Design and Simulation of Engineered Josephson Parametric Amplifier in Quantum Two-Mode Squeezed Radar. 2022. Available online: https://assets-eu.researchsquare.com/files/rs-1948219/v1_covered.pdf (accessed on 10 August 2025).
168. Ludlow, A.D.; Boyd, M.M.; Ye, J.; Peik, E.; Schmidt, P.O. Optical atomic clocks. *Rev. Mod. Phys.* **2015**, *87*, 637–701. [CrossRef]
169. Safronova, M.; Budker, D.; DeMille, D.; Kimball, D.F.J.; Derevianko, A.; Clark, C.W. Search for new physics with atoms and molecules. *Rev. Mod. Phys.* **2018**, *90*, 025008. [CrossRef]
170. Roberts, B.M.; Blewitt, G.; Dailey, C.; Murphy, M.; Pospelov, M.; Rollings, A.; Sherman, J.; Williams, W.; Derevianko, A. Search for domain wall dark matter with atomic clocks on board global positioning system satellites. *Nat. Commun.* **2017**, *8*, 1195. [CrossRef]
171. Borregaard, J.; Sørensen, A.S. Efficient atomic clocks operated with several atomic ensembles. *Phys. Rev. Lett.* **2013**, *111*, 090802. [CrossRef]
172. Appel, J.; Windpassinger, P.J.; Oblak, D.; Hoff, U.B.; Kjærgaard, N.; Polzik, E.S. Mesoscopic atomic entanglement for precision measurements beyond the standard quantum limit. *Proc. Natl. Acad. Sci. USA* **2009**, *106*, 10960–10965. [CrossRef]
173. Braverman, B.; Kawasaki, A.; Vuletić, V. Impact of non-unitary spin squeezing on atomic clock performance. *New J. Phys.* **2018**, *20*, 103019. [CrossRef]
174. Pedrozo-Peñafiel, E.; Colombo, S.; Shu, C.; Adiyatullin, A.F.; Li, Z.; Mendez, E.; Braverman, B.; Kawasaki, A.; Akamatsu, D.; Xiao, Y.; et al. Entanglement on an optical atomic-clock transition. *Nature* **2020**, *588*, 414–418. [CrossRef]
175. Derevianko, A.; Pospelov, M. Hunting for topological dark matter with atomic clocks. *Nat. Phys.* **2014**, *10*, 933–936. [CrossRef]
176. Huang, J.; Zhuang, M.; Lee, C. Entanglement-enhanced quantum metrology: From standard quantum limit to Heisenberg limit. *Appl. Phys. Rev.* **2024**, *11*, 031302. [CrossRef]
177. Yang, W.; Diao, W.; Cai, C.; Wu, T.; Wu, K.; Li, Y.; Li, C.; Duan, C.; Leng, H.; Zi, N.; et al. A bright squeezed light source for quantum sensing. *Chemosensors* **2022**, *11*, 18. [CrossRef]
178. Sheng, D.; Li, S.; Dural, N.; Romalis, M.V. Subfemtotesla scalar atomic magnetometry using multipass cells. *Phys. Rev. Lett.* **2013**, *110*, 160802. [CrossRef]
179. Su, X.; Wang, M.; Yan, Z.; Jia, X.; Xie, C.; Peng, K. Quantum network based on non-classical light. *Sci. China Inf. Sci.* **2020**, *63*, 180503. [CrossRef]
180. Montaña Guerrero, A.; Rincón Celis, R.; Nussenzveig, P.; Martinelli, M.; Marino, A.M.; Florez, H. Continuous variable entanglement in an optical parametric oscillator based on a nondegenerate four wave mixing process in hot alkali atoms. *Phys. Rev. Lett.* **2022**, *129*, 163601. [CrossRef] [PubMed]